

Orbital Order and Fluctuations in Mott Insulators

Giniyat KHALIULLIN^{*)}

*Max-Planck-Institut für Festkörperforschung, Heisenbergstr. 1,
D-70569 Stuttgart, Germany*

Basic mechanisms controlling orbital order and orbital fluctuations in transition metal oxides are discussed. The lattice driven classical orbital picture, e.g. like in manganites LaMnO_3 , is contrasted to the quantum behavior of orbitals in frustrated superexchange models as realised in pseudocubic titanites ATiO_3 and vanadates AVO_3 . In YVO_3 , the lattice and superexchange effects strongly compete — this explains the extreme sensitivity of magnetic states to temperature and doping. Lifting the t_{2g} orbital degeneracy by a relativistic spin-orbital coupling is considered on example of the layered cobaltates. We find that the spin-orbital mixing of low-energy states leads to unusual magnetic correlations in a triangular lattice of the CoO_2 parent compound. Finally, the magnetism of sodium-rich compounds $\text{Na}_{1-x}\text{CoO}_2$ is discussed in terms of a spin/orbital polaronic liquid.

§1. Introduction

It is now well recognized that the orbital degrees of freedom are an important control parameter for physical properties of transition metal oxides.^{1)–3)} The orbital quantum number specifies the electron density distribution in crystal, hence providing a link between magnetism and structure of the chemical bonds.^{4),5)} When the symmetry of the crystal field experienced by a magnetoactive d -electron is high, we encounter the orbital degeneracy problem. In case of a single impurity this degeneracy, being an exact symmetry property, cannot be lifted by orbital-lattice coupling; instead, a purely electronic degeneracy is replaced by the same degeneracy of so-called vibronic states, in which the orbital dynamics and lattice vibrations are entangled and cannot be longer separated. However, the orbital degeneracy must be lifted in a dense system of magnetic ions. The basic physical mechanisms that quench the orbital degrees of freedom in a solid — via the orbital-lattice Jahn-Teller (JT) coupling, via the superexchange (SE) interactions between the orbitals, and via the relativistic spin-orbit coupling — are well known and have extensively been discussed earlier;^{4),5)} see, in particular, a review article.⁶⁾ The purpose of this paper is to discuss some recent developments in the field.

Usually, it is not easy to recognize which mechanism, if any, is dominant in a particular material of interest. As a rule, one expects strong JT interactions for the orbitals of e_g -symmetry as they are directed towards the ligands. On the other hand, Ti, V, Ru, etc., ions with t_{2g} orbital degeneracy are regarded as “weak Jahn-Teller” ions, and the other mechanisms listed above might be equally or even more important in compounds based on these ions. An empirical indication for the strong JT case is a spin-orbital separation in a sense of very different (magnetic T_m and structural T_{str}) transition temperatures and large lattice distortions observed. Or-

^{*)} E-mail: G.Khaliullin@fkf.mpg.de

bitals are (self)trapped by these coherent lattice distortions, and d -shell quadrupole moments are ordered regardless to whether spins are ordered or not. While the other two mechanisms are different in this respect and better characterized, loosely speaking, by spin-orbital confinement indicated by $T_m \simeq T_{str}$. Indeed, strong coupling between spin and orbital orderings/fluctuations is an intrinsic feature of the superexchange and spin-orbit interactions “by construction”. The superexchange mechanism becomes increasingly effective near the Mott metal-insulator transition, because the intensity of virtual charge fluctuations (which are ultimately responsible for the exchange interactions) is large in small charge-gap materials. An increased virtual kinetic energy of electrons near the Mott transition — in other words, the proximity to the metallic state — can make the electronic exchange more efficient in lifting the orbital degeneracy than the electron-lattice coupling.^{7),8)}

As the nature of interactions behind the above mechanisms are different, they usually prefer different orbital states and compete. A quantitative description of the orbital states is thus difficult in general but possible in some limiting cases. In particular, if the ground state orbital polarization is mainly due to strong lattice distortions, one can just “guess” it from the symmetry point of view, as in standard crystal field theory. Low-energy orbital fluctuations are suppressed in this case, and it is sufficient to work with spin-only Hamiltonians operating within the lowest classical orbital state. As an example of such a simple case, we consider in §2 the magnetic and optical properties of LaMnO₃.

The limit of strong (superexchange and relativistic spin-orbital) coupling is more involved theoretically, as one has to start in this case with a Hamiltonian which operates in the full spin-orbital Hilbert space, and derive the ground state spin-orbital wavefunction by optimizing the intersite correlations. It turns out that this job cannot be completed on a simple classical level; one realizes soon that the spin-orbital Hamiltonians possess a large number of classical configurations with the same energy. Therefore, theory must include quantum fluctuations in order to lift the orbital degeneracy and to select the ground state, in which the orbitals and spins can hardly be separated — a different situation to compare with the above case. The origin of such complications lies in the spatial anisotropy of orbital wavefunctions. This leads to a specific, non-Heisenberg form of the orbital interactions which are frustrated on high-symmetry lattices containing several equivalent bond directions. Physically, orbital exchange interactions on different bonds require the population of different orbital states and hence compete. This results in an infinite degeneracy of the classical ground states. A substantial part of this paper is devoted to illustrate how the orbital frustration is resolved by quantum effects in spin-orbital models, and to discuss results in the context of titanites and vanadates with perovskite structure (§3). We will also demonstrate a crucial difference in the low-energy behavior of superexchange models for e_g and t_{2g} orbitals.

In some cases, the competition between the superexchange and orbital-lattice interactions result in a rich phase diagram, including mutually exclusive states separated by first order transitions. A nice example of this is YVO₃ discussed in §4. In particular, we show how a competition between the three most relevant spin/orbital electronic phases is sensitively controlled in YVO₃ by temperature or small amounts

of hole-doping.

The last part of the paper, §5, discusses the role of the relativistic spin-orbit coupling λ_{so} , which effectively reduces the orbital degeneracy already on the single-ion level. This coupling mixes-up the spin and orbital quantum numbers in the ground state wavefunction, such that the magnetic ordering implies both the orbital and spin ordering at once. The spin-orbit coupling mechanism might be essential in insulating compounds of late- $3d$ ions with large λ_{so} and also in $4d$ -ruthenates. We focus here on two-dimensional cobaltates with a triangular lattice, and present a theory which shows that very unusual magnetic states can be stabilized in CoO_2 planes by spin-orbit coupling. We also discuss in that section, how the orbital degeneracy and well known spin-state flexibility of cobalt ions lead to a polaron-liquid picture for the sodium-rich compounds $\text{Na}_{1-x}\text{CoO}_2$, and explain their magnetic properties.

Our intention is to put more emphasis on a comparative discussion of different mechanisms of lifting the orbital degeneracy, by considering their predictions in the context of particular compounds. Apart from discussing previous work, the manuscript presents many original results which either develop known ideas or are completely new. These new results and predictions made may help to resolve controversial issues and to discriminate between the different models and viewpoints.

§2. Lifting the orbital degeneracy by lattice distortions

Let us consider the Mott insulators with composition ABO_3 , where A and B sites accommodate the rare-earth and transition metal ions, respectively. They crystallize in a distorted perovskite structure.^{1),9)} Despite a very simple, nearly cubic lattice formed by magnetic ions, a variety of spin structures are observed in these compounds: An isotropic G -type antiferromagnetism (AF) in LaTiO_3 , isotropic ferromagnetism (F) in YTiO_3 , and also anisotropic magnetic states such as C -type AF in LaVO_3 and A -type AF in LaMnO_3 .*) The richness of the spin-orbital states, realized in these compounds with a similar lattice structure, already indicates that different mechanisms lifting the orbital degeneracy might be at work, depending on the type of orbitals, the spin value, and on the closeness to the Mott transition.

Considering the lattice distortions in perovskites, one should distinguish distortions of two different origins: (A) The first one is due to ionic-size mismatch effects, that generate cooperative rotations and also some distortions of octahedra in order to fulfill the close-packing conditions within a perovskite structure. These are the “extrinsic” deviations from cubic symmetry, in a sense that they are not triggered by orbitals themselves and are present even in perovskites having no orbital degeneracy at all, e.g. in LaAlO_3 or LaFeO_3 . The orbitals may split and polarize under the extrinsic deformations, but they play essentially the role of spectators, and to speak of “orbital ordering” in a sense of cooperative phenomenon (such as “spin ordering”) would therefore be misleading in this case. (B) Secondly, cooperative JT-distortions, which are generated by orbital-lattice coupling itself at the orbital

*) G -type AF structure: spins are staggered in all three directions. C -type (A -type) structure consists of ferromagnetic chains (planes) with AF order between them.

ordering temperature (seen by “eyes” as a structural transition).

Usually, these two contributions are superimposed on each other. Sometimes, it is not easy to identify which one is dominant. The temperature dependence of the distortion is helpful in this context. Manganites show an orbital order-disorder phase transition at high temperatures at about 800 K, below which a large, of the order of 15%, distortion of octahedra sets in. This indicates the dominant role of a cooperative JT physics, which is natural for e_g orbital systems with strong coupling between the oxygen vibrations and e_g quadrupole. In contrast, no *cooperative* structural phase transition has thus far been observed in titanates, suggesting that small lattice distortions present in these compounds are mostly due to the ionic-size mismatch effects. This seems also plausible, as t_{2g} -orbital JT coupling is weak.

Whatever the origin, the lattice distortions generate low (noncubic) symmetry components in the crystal field potential, which split the initially degenerate orbital levels. While structure of the lowest, occupied crystal-field level can be determined without much problem — simply by symmetry considerations, the level splittings are very sensitive to the value of (i) distortions and (ii) the orbital-lattice coupling (both factors being much smaller in t_{2g} orbital compounds). If the splittings are large enough to localize electrons in the lowest crystal-field level and to suppress the inter-site orbital fluctuations, classical treatment of orbitals is justified. Accordingly, the e_g -electron density is determined by a function parameterized via the site-dependent classical variables α_i :

$$\psi_i = \cos \alpha_i |3z^2 - r^2 \rangle + \sin \alpha_i |x^2 - y^2 \rangle, \quad (2.1)$$

while the occupied t_{2g} orbital can be expressed via the two angles:

$$\psi_i = \cos \alpha_i |xy \rangle + \sin \alpha_i \cos \beta_i |yz \rangle + \sin \alpha_i \sin \beta_i |zx \rangle. \quad (2.2)$$

A knowledge of these functions allows one to express a various experimental observables such as spin interactions, optical absorption and Raman scattering intensities, etc., in terms of a few “orbital angles”. [In general, classical orbital states may include also a complex wave-functions, but they are excluded in the case of strong lattice distortions^{4),6)}.] These angles can thus be determined from the experimental data, and then compared with those suggested by a crystal-field theory. Such a classical approach is a great simplification of the “orbital physics”, and it has widely and successfully been used in the past. Concerning the orbital excitations in this picture, they can basically be regarded as a nearly localized transitions between the crystal-field levels. We demonstrate below how nicely this canonical “orbital-angle” scenario does work in manganites, and discuss its shortcomings in titanites and vanadates.

2.1. e_g orbitals: The case of $LaMnO_3$

Below a cooperative JT phase transition at $\sim 800 \text{ K} \gg T_N$, a two-sublattice orbital order sets in. Suggested by C-type arrangement of octahedron elongation (staggered within ab planes and repeated along c direction), the lowest crystal field level can be parameterized via the orbital angle θ ⁵⁾ as follows:

$$|\pm \rangle = \cos \frac{\theta}{2} |3z^2 - r^2 \rangle \pm \sin \frac{\theta}{2} |x^2 - y^2 \rangle. \quad (2.3)$$

In this state, the e_g electron distribution is spatially asymmetric, which leads to strong anisotropy in spin exchange couplings and optical transition amplitudes. Thus, the orbital angle θ can be determined from a related experiments and compared with $\theta \sim 108^\circ$ ⁵⁾ suggested by structural data.

Spin interactions. — For manganites, there are several intersite virtual transitions $d_i^4 d_j^4 \rightarrow d_i^3 d_j^5$, each contributing to the spin-orbital superexchange. The corresponding energies can be parameterized via the Coulomb repulsion $U = A + 4B + 3C$ for electrons residing in the same e_g orbital ($U n_{\alpha\uparrow} n_{\alpha\downarrow}$), the Hund's integral $J_H = 4B + C$ between e_g spins in different orbitals ($-2J_H \vec{s}_\alpha \cdot \vec{s}_\beta$), the Hund's integral $J'_H = 2B + C$ between the e_g spin and the t_{2g} -core spin ($-2J'_H \vec{S}_t \cdot \vec{s}_e$), and, finally, the Jahn-Teller splitting Δ_{JT} between different e_g -orbitals: $\Delta_{JT}(n_\beta - n_\alpha)/2$. (A, B, C are the Racah parameters, see Ref. 10) for details.) For the e_g electron hopping $d_i^4 d_j^4 \rightarrow d_i^3 d_j^5$, we obtain the following five different transition energies:

$$\begin{aligned} E_1 &= U + \Delta_{JT} - 3J_H, \\ E_2 &= U + \Delta_{JT} - 3J_H + 5J'_H, \\ E_3 &= U + \Delta_{JT} + 3J'_H - \sqrt{\Delta_{JT}^2 + J_H^2}, \\ E_4 &= U + \Delta_{JT} + 3J'_H - J_H, \\ E_5 &= U + \Delta_{JT} + 3J'_H + \sqrt{\Delta_{JT}^2 + J_H^2}. \end{aligned} \quad (2.4)$$

There are also (weaker) transitions associated with t_{2g} electron hoppings, which provide an isotropic AF coupling between the spins $J_t(\vec{S}_i \cdot \vec{S}_j)$, with $J_t = t'^2/2E_t$ and $S = 2$ of Mn^{3+} . Here, $E_t = U + J_H + 2J'_H$ is an average excitation energy for the intersite t_{2g} -electron hoppings, and $t' \simeq t/3$ follows from the Slater-Koster relation.

From a fit to the optical conductivity in LaMnO_3 , the energies E_n have been obtained.¹¹⁾ Then, it follows from Eqs. (2.4) that $U \sim 3.4$ eV, $J'_H \sim 0.5$ eV, $J_H \sim 0.7$ eV and $\Delta_{JT} \sim 0.7$ eV (in the present notations for U , J'_H , J_H given above; Ref. 11) used instead $\tilde{U} = A - 2B + 3C$ and $\tilde{J}_H = 2B + C$). The Hund's integrals are somewhat reduced from the atomic values $J'_H = 0.65$ eV and $J_H = 0.89$ eV.¹⁰⁾ The e_g -orbital splitting is substantial, suggesting that orbitals are indeed strongly polarized by static JT distortions, and justifying a crystal-field approach below 800 K. A large JT binding energy ($= \Delta_{JT}/4$) also indicates that dynamical distortions of octahedra are well present above 800 K, thus a structural transition is of the order-disorder type for these distortions and e_g -quadrupole moments. This is in full accord with a view expressed in Ref. 12). Note, however, that JT energy scales are smaller than those set by correlations, thus LaMnO_3 has to be regarded as a typical Mott insulator.

The superexchange Hamiltonian H consists of several terms, $H_n^{(\gamma)}$, originating from virtual hoppings with energies E_n (2.4) in the intermediate state (γ denotes the bond directions a, b, c). Following the derivation of Ref. 13), we obtain:

$$\begin{aligned} H_{ij}^{(\gamma)} &= \frac{t^2}{20} \left[-\frac{1}{E_1} (\vec{S}_i \cdot \vec{S}_j + 6)(1 - 4\tau_i \tau_j)^{(\gamma)} + \left(\frac{3}{8E_2} + \frac{5}{8E_4} \right) (\vec{S}_i \cdot \vec{S}_j - 4)(1 - 4\tau_i \tau_j)^{(\gamma)} \right. \\ &\quad \left. + \left(\frac{5}{8E_3} + \frac{5}{8E_5} \right) (\vec{S}_i \cdot \vec{S}_j - 4)(1 - 2\tau_i)^{(\gamma)}(1 - 2\tau_j)^{(\gamma)} \right], \end{aligned} \quad (2.5)$$

where the e_g -pseudospins $\tau^{(\gamma)}$ are defined as $2\tau_i^{(c)} = \sigma_i^z$, $2\tau_i^{(a)} = \cos\phi\sigma_i^z + \sin\phi\sigma_i^x$, $2\tau_i^{(b)} = \cos\phi\sigma_i^z - \sin\phi\sigma_i^x$ with $\phi = 2\pi/3$. Here, σ^z and σ^x are the Pauli matrices, and $\sigma^z = 1$ (-1) corresponds to a $|x^2 - y^2\rangle$ ($|3z^2 - r^2\rangle$) state. Note that no σ^y -component is involved in $\tau^{(\gamma)}$ operators; this reflects the fact that the orbital angular momentum is fully quenched within the e_g doublet. Physically, a pseudospin $\tau^{(\gamma)}$ -structure of Eq. (2.5) reflects the dependence of spin interactions on the orbitals that are occupied, expressing thereby a famous Goodenough-Kanamori rules in a compressed formal way.⁶⁾

In a classical orbital state (2.3), operators σ^α can be regarded as a numbers $\sigma^z = -\cos\theta$ and $\sigma^x = \pm\sin\theta$, thus we may set $(1 - 4\tau_i\tau_j)^{(c)} = \sin^2\theta$, $(1 - 4\tau_i\tau_j)^{(ab)} = (3/4 + \sin^2\theta)$, etc., in Eq. (2.5). At this point, the spin-orbital model (2.5) ‘‘collapses’’ into the Heisenberg Hamiltonian, $J_\gamma(\theta)(\vec{S}_i \cdot \vec{S}_j)$, and only ‘‘memory’’ of orbitals that is left is in a possible anisotropy of spin-exchange constants $J_{a,b,c}$:

$$\begin{aligned} J_c &= \frac{t^2}{20} \left[\left(-\frac{1}{E_1} + \frac{3}{8E_2} + \frac{5}{8E_4} \right) \sin^2\theta + \frac{5}{8} \left(\frac{1}{E_3} + \frac{1}{E_5} \right) (1 + \cos\theta)^2 \right] + J_t, \\ J_{ab} &= \frac{t^2}{20} \left[\left(-\frac{1}{E_1} + \frac{3}{8E_2} + \frac{5}{8E_4} \right) \left(\frac{3}{4} + \sin^2\theta \right) + \frac{5}{8} \left(\frac{1}{E_3} + \frac{1}{E_5} \right) \left(\frac{1}{2} - \cos\theta \right)^2 \right] + J_t. \end{aligned} \quad (2.6)$$

Note that the E_1 -term has a negative (ferromagnetic) sign. This corresponds to the high-spin intersite transition with the lowest energy E_1 , which shows up in optical absorption spectra as a separate band near 2 eV.¹¹⁾ From the spectral weight of this line, one can determine the value of t , see below. All the other terms come from low-spin transitions. The orbital angle θ controls the competition between a ferromagnetic E_1 -term and AF E_2, \dots, E_5 -contributions in a bond-selective way.

Optical intensities. — Charge transitions $d_i^4 d_j^4 \rightarrow d_i^3 d_j^5$ are optically active. The spectral shape of corresponding lines are controlled by band motion of the excited doublons (holes) in the upper (lower) Hubbard bands and by their excitonic binding effects. The intensity of each line at E_n is determined by a virtual kinetic energy, and thus, according to the optical sum rule, can be expressed via the expectation values of superexchange terms $H_n^{(\gamma)}(ij)$ for each bond direction γ .

The optical intensity data is often quantified via the effective carrier number,

$$N_{eff,n}^{(\gamma)} = \frac{2m_0v_0}{\pi e^2} \int_0^\infty \sigma_n^{(\gamma)}(\omega) d\omega, \quad (2.7)$$

where m_0 is the free electron mass, and $v_0 = a_0^3$ is the volume per magnetic ion. Via the optical sum rule applied to a given transition with $n = 1, \dots, 5$, the value of $N_{eff,n}^{(\gamma)}$ can be expressed as follows:¹⁴⁾

$$N_{eff,n}^{(\gamma)} = \frac{m_0 a_0^2}{\hbar^2} K_n^{(\gamma)} = -\frac{m_0 a_0^2}{\hbar^2} \langle 2H_n^{(\gamma)}(ij) \rangle. \quad (2.8)$$

Here, $K_n^{(\gamma)}$ is the kinetic energy gain associated with a given virtual transition n for a bond $\langle ij \rangle$ along axis γ . The second equality in this expression states that $K_n^{(\gamma)}$,

hence the intensity of a given optical transition, is controlled by expectation value of the corresponding term $H_n^{(\gamma)}$ in spin-orbital superexchange interaction (2.5). Via the operators $\tau^{(\gamma)}$, each optical transition E_n obtains its own dependence on the orbital angle θ . Thus, Eq. (2.8) forms a basis for the study of orbital states by means of optical spectroscopy, in addition to the magnetic data. Using a full set of the optical and magnetic data, it becomes possible to quantify more reliably the values of t , U , J_H in crystal, and to determine the SE-energy scale, as it has been proposed in Ref. 14), and worked out specifically for LaVO_3 ¹⁴⁾ and LaMnO_3 .¹¹⁾

Physically, spin and orbital correlations determine the optical intensities of different transitions E_n via the selection rules, which are implicit in Eq. (2.5). For instance, the intensity of the high-spin transitions obtained from the E_1 -term in Eq. (2.5) reads:

$$\begin{aligned} K_1^{(c)} &= \frac{t^2}{10E_1} \langle \vec{S}_i \cdot \vec{S}_j + 6 \rangle^{(c)} \sin^2 \theta , \\ K_1^{(ab)} &= \frac{t^2}{10E_1} \langle \vec{S}_i \cdot \vec{S}_j + 6 \rangle^{(ab)} (3/4 + \sin^2 \theta) . \end{aligned} \quad (2.9)$$

At $T \ll T_N \sim 140$ K, $\langle \vec{S}_i \cdot \vec{S}_j \rangle^{(ab)} \Rightarrow 4$ and $\langle \vec{S}_i \cdot \vec{S}_j \rangle^{(c)} \Rightarrow -4$ for the A -type classical spin state, while $\langle \vec{S}_i \cdot \vec{S}_j \rangle \Rightarrow 0$ at $T \gg T_N$. Thus, both spin and orbital correlations induce a strong polarization and temperature dependence of the optical conductivity. Note, that the e_g -hopping integral t determines the overall intensity; we find that $t \simeq 0.4$ eV fits well the observed optical weights.¹¹⁾ This gives $4t^2/U \simeq 190$ meV (larger than in cuprates, since t stands here for the $3z^2 - r^2$ orbitals and thus is larger than a planar $x^2 - y^2$ orbital-transfer).

A quantitative predictions of the above ‘‘orbital-angle’’ theory for spin-exchange constants and optical intensities, expressed in Eqs. (2.6) and (2.9) solely in terms of a classical variable θ , have nicely been confirmed in Ref. 11). It is found that the angle $\theta = 102^\circ$ well describes the optical anisotropy, and gives the exchange integrals $J_c = 1.2$ meV, $J_{ab} = -1.6$ meV in perfect agreement with magnon data.¹⁵⁾ Given that ‘‘the lattice angle’’ 108° has been estimated from the octahedron distortions alone, and thus may slightly change in reality by GdFeO_3 -type distortions and exchange interactions, one may speak of a quantitative description of the entire set of data in a self-contained manner (everything is taken from the experiment). This implies the dominant role of (JT) lattice distortions in lifting the orbital degeneracy in manganites as expected. Of course, the situation changes if one injects a mobile holes, or drives a system closer to the Mott transition. The orbital order is indeed suppressed in LaMnO_3 under high pressure,¹⁶⁾ in spite the insulating state is still retained. Pressure reduces the ionic-size mismatch effects, and, more importantly, decreases the charge gap and thus enhances the kinetic energy. The latter implies an increased role of superexchange interactions which, as discussed later, are strongly frustrated on cubic lattices; consequently, a classical orbital order is degraded. In addition, a weak e_g -density modulation like in case of CaFeO_3 ¹⁾ may also contribute to the orbital quenching near the metal-insulator transition.

2.2. t_{2g} orbitals: Titanates

Depending on the A-site ion radius, two types of magnetic orderings have thus far been identified in ATiO_3 compounds: (I) G -type AF state as in LaTiO_3 , which changes to (II) ferromagnetic ordering for the smaller size A-ions as in YTiO_3 , with strong suppression of transition temperatures in between.¹⁷⁾ Surprisingly enough, both AF and F states are isotropic in a sense of equal exchange couplings in all three crystallographic directions.^{18),19)} Such a robust isotropy of spin interactions (despite the fact that the c -direction bonds are structurally not equivalent to those in the ab plane), and a kind of “soft” (instead of strong first order) transition between such a incompatible spin states is quite unusual.

Another unique feature of titanites is that, different from many oxides, no cooperative structural phase transition is observed so far in LaTiO_3 and YTiO_3 . (Except for a sizable magnetostriction in LaTiO_3 ,²⁰⁾ indicating the presence of low-energy orbital degeneracy.) This is very unusual because the JT physics could apparently be anticipated for Ti^{3+} ions in nearly octahedral environment. One way of thinking of this paradox is that^{18), 7), 8), 19), 21), 22)} the titanites are located close to the Mott transition, and the enhanced virtual charge fluctuations, represented usually in the form of spin-orbital superexchange interactions, frustrate and suppress expected JT-orbital order (see next section). Yet another explanation is possible,^{23), 20)} which is based on local crystal field picture. In this view, the orbital state is controlled by lattice, instead of superexchange interactions. Namely, it is thought that extrinsic lattice distortions caused by ionic-size mismatch effects (so-called GdFeO_3 -type distortions) remove the orbital degeneracy for all temperatures, thus orbital dynamics is suppressed and no Jahn-Teller instability can develop, either. One caveat in this reasoning, though, is that a cooperative orbital transitions are *not prevented* by GdFeO_3 -distortions (of the similar size) in other t_{2g} compounds, e.g. in pseudocubic vanadates. Thus, the titanites seem to be unique and require other than the “ GdFeO_3 -explanation” for the orbital quenching. Nonetheless, let us consider now in more detail the predictions of such a crystal-field scenario, that is, the “orbital-angle” picture expressed in Eq. (2.2).

The perovskite structure is rather “tolerant” and can accommodate a variation of the A-site ionic radius by cooperative rotations of octahedra. This is accompanied by a shift of A-cations such that the distances A–O and A–Ti vary somewhat. Also the oxygen octahedra get distorted, but their distortion ($\sim 3\%$) is far less than that of the oxygen coordination around the A-cation. The nonequivalence of the Ti–A distances and weak distortions of octahedra induce then a noncubic crystal field for the Ti-ion. In LaTiO_3 , the octahedron is nearly perfect, but the Ti–La distance along one of the body diagonals is shorter,²⁰⁾ suggesting the lowest crystal-field level of $\sim |xz + yz \pm xy\rangle/\sqrt{3}$ symmetry, as has been confirmed in Refs. 23) and 20) by explicit crystal-field calculations. This state describes an orbital elongated along the short La–Ti–La diagonal, and the sign (\pm) accounts for the fact that the short diagonal direction alternates along the c -axis (reflecting a mirror plane present in crystal structure). Thus, lattice distortions impose the orbital pattern of A -type structure. In YTiO_3 , the A-site shifts and concomitant distortions of octahedra,

induced²⁴⁾ by ionic-size mismatch effects including A–O and A–Ti covalency, are stronger. A crystal-field^{23), 20)} and band structure^{25), 26)} calculations predict that these distortions stabilize a four-sublattice pattern of planar orbitals

$$\psi_{1,3} \sim |xz \pm xy\rangle/\sqrt{2} \quad \text{and} \quad \psi_{2,4} \sim |yz \pm xy\rangle/\sqrt{2} . \quad (2.10)$$

Note that xy orbitals are more populated (with two times larger filling-factor when averaged over sites). This state would therefore lead to a sizable anisotropy of the electronic properties. We recall that all the above orbital patterns are nearly temperature independent, since *no cooperative JT* structural transition (like in manganites) is involved here.

Earlier neutron diffraction²⁷⁾ and NMR²⁸⁾ experiments gave support to the crystal-field ground states described above; however, this has recently been reconsidered in Ref. 29). Namely, NMR-spectra in YTiO₃ show that the t_{2g} -quadrupole moment is in fact markedly reduced from the predictions of crystal-field theory, and this has been attributed to quantum orbital fluctuations.²⁹⁾ On the other hand, this may be not easy to reconcile with the earlier “no orbital-fluctuations” interpretation of NMR spectra in *less distorted* LaTiO₃,²⁸⁾ — thus no final conclusion can be made at present from NMR data alone.³⁰⁾

For the *first-principle* study of effects of lattice distortions on the orbital states in titanites, we refer to the recent work³¹⁾ in which: the ground-state orbital polarization, (crystal-field) energy level structure, and spin exchange interactions have been calculated within the LDA+DMFT framework. In this study, which attempts to combine a quantum chemistry with strong correlations, a nearly complete condensation of electrons in a particular single orbital (an elongated, of the a_{1g} type in LaTiO₃ and a planar one in YTiO₃, as just discussed) is found, in accord with a simpler crystal-field calculations of Refs. 23) and 20). Other (empty) orbital levels are found to be located at energies as high as ~ 200 meV; this qualitatively agrees again with Refs. 20) and 23), but deviates from the predictions of yet another first-principle study of Ref. 32). The calculations of Ref. 31) give correct spin ordering patterns for both compounds (for a first time, to our knowledge; — usually, it is difficult to get them both right simultaneously, see Ref. 32)). However, the calculated spin exchange constants: $J_c = -0.5$ meV, $J_{ab} = -4.0$ meV for YTiO₃, and $J_c = 5.0$ meV, $J_{ab} = 3.2$ meV for LaTiO₃, — as well as their anisotropy ratio J_c/J_{ab} are quite different from the observed values: $J_c \simeq J_{ab} \simeq -3$ meV (YTiO₃¹⁹⁾) and $J_c \simeq J_{ab} \simeq 15.5$ meV (LaTiO₃¹⁸⁾). Large anisotropy of the calculated spin couplings $J_c/J_{ab} \sim 0.1$ in YTiO₃ is particularly disturbing; the same trend is found in Ref. 32): $J_c/J_{ab} \sim 0.3$. The origin of anisotropy is — put it simple way — that the lattice distortions make the c -axis structurally different from the two others, and this translates into $J_c \neq J_{ab}$ within a crystal-field picture. In principle, one can achieve $J_c/J_{ab} = 1$ by tuning the orbital angles and J_H by “hand”, but, as demonstrated in Ref. 19), this is highly sensitive procedure and seems more like as an “accident” rather than explanation. Given that the degree of lattice distortions in LaTiO₃ and YTiO₃ are different²⁰⁾ — as reflected clearly in their very different crystal-field states — the observation $J_c/J_{ab} \simeq 1$ in *both of them* is enigmatic, and the results of first-principle calculations make the case complete.

A way to overcome this problem is — as proposed in Refs. 18) and 19) on physical grounds — to relax the orbital polarization: this would make the spin distribution more isotropic. In other words, we abandon the fixed orbital states like Eq. (2-10), and let the orbital angles to fluctuate, as they do in case of a dynamical JT problem. However, a dynamical aspects of JT physics as well as the intersite superexchange fluctuations are suppressed by a static crystal-field splittings, which, according to Ref. 24), are large: the t_{2g} level structure reads as [0, 200, 330] meV in YTiO_3 , and [0, 140, 200] meV in LaTiO_3 .

Such a strong noncubic splitting of t_{2g} triplet, exceeding 10% of the cubic $10Dq \sim 1.5\text{--}2.0$ eV is quite surprising, and, in our view, is overestimated in the calculations. Indeed, e_g orbital splitting in manganites has been found ~ 0.7 eV (see above) which is about 30% of $10Dq$; this sounds reasonable because of (i) very large octahedron distortions ($\sim 15\%$) that (ii) strongly couple to the e_g -quadrupole. Both these factors are much smaller in titanates: (i) octahedron distortions are about 3% only, while effects of further neighbors should be screened quite well due to a proximity of metallicity; (ii) coupling to the t_{2g} -quadrupole is much less than that for e_g — otherwise a cooperative JT transition would take place followed by a strong distortions like in manganites. Putting these together, we “estimate” that a t_{2g} splitting should be at least by an order of value less than that seen for e_g level in manganites, — that is, well below 100 meV. This would make it possible that orbitals start talking to spins and fluctuate as suggested in Ref. 7).

In general, a quantitative calculation of the level splittings in a solid is a rather sensitive matter (nontrivial even for well localized f -electrons). Concerning a numerical calculations, we tend to speculate that a notion of “orbital splitting” (as used in the models) might be not that well defined in first-principle calculations, which are designed to obtain the ground state properties (but not excitation spectra). This might be a particularly delicate matter in a strongly correlated systems, where effective orbital splittings may have strong t/U and frequency dependences.³³⁾ As far as a simple crystal-field calculations are concerned, they are useful for symmetry analyses but, quantitatively, often strongly deviate from what is observed. As an example of this sort, we refer to the case of Ti^{3+} ions in a Al_2O_3 host, where two optical transitions within a t_{2g} multiplet have directly been observed.³⁴⁾ The level splitting ~ 13 meV found is astonishingly small, given a sizable (more than 5%) distortion of octahedron. A strong reduction of the level splitting from a static crystal-field model has been attributed to the orbital dynamics (due to the dynamical JT effect, in that case).

As a possible test of a crystal-field calculations in perovskites, it should be very instructive to perform a similar work for LaVO_3 and YVO_3 at room temperature. The point is that there is a *cooperative, of second order* orbital phase transition in vanadates at low-temperature (below 200 K). To be consistent with this observation, the level-spacings induced by GdFeO_3 -type, etc., distortions (of the similar size as in titanites) must come out very small.

Whatever the scenario, the orbital excitations obtain a characteristic energy scale set by the most relevant interactions. However, the predictions of a local crystal-field theory and a cooperative SE interactions for the momentum and polarization

dependences of orbital response are radically different. Such a test case has recently been provided by the Raman light scattering from orbital excitations in LaTiO_3 and YTiO_3 , see Ref. 35). In short, it was found that the polarization rules, dictated by a crystal-field theory, are in complete disagreement with those observed. Instead, the intensity of the Raman scattering obeys the cubic symmetry in both compounds when the sample is rotated. Altogether, magnon and Raman data reveal a universal (cubic) symmetry of the spin and orbital responses in titanites, which is seemingly not sensitive to the differences in their lattice distortions. Such a universality is hard to explain in terms of a crystal-field picture based — by its very meaning — on the deviations away cubic symmetry.

Moreover, a picture based on a Heisenberg spins residing on a fully polarized single orbital has a problem in explaining the anomalous spin reduction in LaTiO_3 .¹⁸⁾ The magnetic moment measured is as small as $M \simeq 0.5\mu_B$, so the deviation from the nearest-neighbor 3D Heisenberg model value $M_H \simeq 0.84\mu_B$ is unusually large: $\delta M/M_H = (M_H - M)/M_H \sim 40\%$. As a first attempt to cure this problem, one may notice that the Heisenberg spin system is itself derived from the Hubbard model by integrating out virtual charge fluctuations (empty and doubly occupied states). Therefore, the amplitude of the physical magnetic moment is reduced from that of the low-energy Heisenberg model via $M_{ph} = M_H(1 - n_h - n_d)$. However, this reduction is in fact very small, as one can see from the following argument. Let us discard for a moment the orbital fluctuations, and consider a single orbital model. By second-order perturbation theory, densities of the virtual holons n_h and doublons n_d , generated by electron hoppings in a Mott insulator, can be estimated as $n_h = n_d \simeq z(\frac{t}{U})^2$, where z is the nearest-neighbor coordination number. Thus, the associated moment reduction is $\delta M/M_H \simeq \frac{1}{2z}(\frac{2zt}{U})^2$. Even near the metal-insulator transition, that is for $U \simeq 2zt$, this gives in 3D cubic lattice $\delta M/M_H \simeq \frac{1}{2z} \simeq 8\%$ only. (We note that this simple consideration is supported by 2D Hubbard model calculations of Ref. 36): the deviation of the staggered moment from 2D Heisenberg limit was found $\delta M/M_H \simeq 12\%$ at $U \simeq 8t$, in perfect agreement with the above $1/2z$ -scaling.) This implies that the anomalous moment reduction in LaTiO_3 requires some extra physics not contained in a single-orbital Hubbard or Heisenberg models. (In fact, an “extra” moment reduction is always present whenever orbital fluctuations are suspected: LaTiO_3 , LaVO_3 and C -phase of YVO_3 .) Enhanced spin fluctuations, a spatial isotropy of the spin exchange integrals, and similar cubic symmetry found in the Raman scattering from orbital fluctuations strongly suggest multiband effects, that is, the presence of orbital quantum dynamics in the ground state of titanites.

2.3. t_{2g} orbitals: Vanadates

In vanadium oxides AVO_3 one is dealing with a t_{2g}^2 configuration, obtained by a removal of an electron from the t_{2g}^3 shell which is orbitally-nondegenerate (because of the Hund’s rule). From a viewpoint of the JT physics, this represents a hole-analogy of titanites: One hole in the t_{2g} manifold instead of one electron in ATiO_3 . Similar to the titanites, they crystallize in a perovskite structure, with GdFeO_3 -type distortions increasing from La- towards Y-based compounds, as usual. At lower temperatures, vanadates undergo a cooperative structural transition (of second-order,

typically). This very fact indicates the presence of unquenched low-energy orbital degeneracy, suggesting that underlying GdFeO₃-type distortions are indeed not sufficient to remove it. The structural transition temperature T_{str} is nearly confined to the magnetic one $T_N \sim 140$ K in LaVO₃ — the relation $T_{str} \sim T_N$ holds even in a hole-doped samples,³⁷⁾ — while $T_{str} \sim 200$ K in YVO₃ is quite separated from $T_N \sim 120$ K. It is accepted that the xy orbital is static below T_{str} and accommodates one of the two magnetic electrons. An empirical correlation between T_{str} and the A-site ionic size suggests that GdFeO₃-type distortions “help” this stabilization.

However, a mechanism lifting the degeneracy of xz/yz doublet is controversial: Is it also of lattice origin, or controlled by the superexchange? Based on distortions of octahedra (albeit as small as in YTiO₃), many researchers draw a pattern of staggered orbitals polarized by JT interactions. This way of thinking is conceptually the same as in manganites (the only difference is the energy scales): a cooperative, three-dimensional JT-ordering of xz/yz doublets. However, this leaves open the questions: Why is the JT mechanism so effective for the t_{2g} -hole of vanadates, while being apparently innocent (no structural transition) in titanites with one t_{2g} -electron? Why is the T_{str} , if driven by JT physics, so closely correlated with T_N in LaVO₃? Motivated by these basic questions, we proposed a while ago a different view,³⁸⁾ which attributes the difference between vanadates and titanites to the different spin values: classical $S = 1$ versus more quantum $S = 1/2$. Being not much important for JT-physics, the spin-value is of key importance for the superexchange mechanism of lifting the orbital degeneracy. An apparent correlation between T_{str} and T_N in LaVO₃, the origin of C -type spin pattern (different from titanites), etc., all find a coherent explanation within the model of Ref. 38). This theory predicts that the xy orbital becomes indeed classical (as commonly believed) below T_{str} , but, different from the JT scenario, xz/yz doublets keep fluctuating and their degeneracy is lifted mainly due to the formation of quasi-1D orbital chains with Heisenberg-like dynamics. Concerning the separation of T_{str} from T_N in YVO₃, we think it is due to an increased tendency for the xy orbital-selection by GdFeO₃-type distortions; this helps in fact the formation of xz/yz doublets already above T_N . Below T_{str} , a short-range spin correlations and orbital dynamics is of quasi 1D nature, and xz/yz doublet polarization is small. Essentially, the xz/yz sector remains almost disordered for both quantum and entropy reasons.^{38)–40)} In our view, a complete classical order in the xz/yz sector sets in only below a second structural transition at $T_{str}^* \sim 77$ K, determined by a competition between ~ 1 D spin-orbital physics and GdFeO₃-type distortions, which prefer a different ground state (more to come in §4).

Apart from a neutron scattering experiments³⁹⁾ challenging a classical JT picture for vanadates, we would like to quote here a recent paper,⁴¹⁾ which observes that the vanadates become “transparent” for the thermal phonons *only* below a second transition at T_{str}^* (if present), in a so-called low-temperature G -phase, where we indeed expect that everything should be “normal” (described by a static orbital-angle physics). Enhanced phonon scattering on xz/yz fluctuations, which suddenly disappears below T_{str}^* , is very natural within the superexchange model. While it would be hard to understand this, if the orbital states both above and below T_{str}^* are classically ordered via the JT mechanism. Obviously, the thermal conductivity

measurements are highly desired in titanites, in order to see as whether the phonon scattering remains unquenched down to low temperatures as expected from a superexchange picture, or will be like in manganites with a static orbitals.

To summarize our present view on the role of orbital-lattice mechanism in perovskites: (i) The JT physics dominates in manganites, with a secondary role of SE interactions and extrinsic GdFeO₃-type distortions; (ii) In titanites and vanadates, the “orbital-angle” description is insufficient. It seems that orbital-lattice coupling plays a secondary, but *important* role providing a phase-selection out of a manifold of nearly degenerate many-body quantum states, offered by superexchange interactions. In vanadates with smaller A-site ions, though, a classical *G* phase, favored by GdFeO₃-type distortions, takes over in the ground state, but the quantum spin-orbital states are restored again at finite temperature due to their larger spin-orbital entropy;^{38),39)} — a somewhat curious cooperation of quantum and thermal effects.

§3. Lifting the orbital degeneracy by spin-orbital superexchange

While the kinetic energy of electrons is represented in metals by the hopping *t*-Hamiltonian, it takes a form of spin-orbital superexchange in the Mott insulator. The superexchange interactions are obtained by eliminating the virtual doublon/holon states, a procedure which is justified as far as t/U is small, and the resulting SE-scale $4t^2/U$ is smaller than *t* itself. Near the Mott transition, a longer-range coupling and retardation effects, caused by a softening and unbinding of doublon/holon excitations are expected, and separation of the spin-orbital modes from an emergent low-energy charge and fermionic excitations becomes valid only locally. An example for the latter case is a cubic perovskite SrFeO₃, “bad” metal which is located just slightly below the Mott transition, or CaFeO₃ having in addition a weak charge-density modulation of low-energy holons/doublons. Here, both the superexchange interaction accounting for the high-energy charge fluctuations, *and* the low-energy/gapless charge excitations present near the transition, have to be considered on equal footing.⁴²⁾ This picture leads to a strong competition between the superexchange and double-exchange processes, resulting in orbital disorder, a helical spin structure, and small-only Drude weight (quantifying the distance to the Mott-transition), as observed in ferrates.⁴³⁾

We consider here conventional nearest-neighbor (NN) SE-models, assuming that the above criteria $4t^2/U < t$ is valid and the local spin-orbital degrees of freedom are protected by a charge gap. This is in fact consistent with spinwave measurements,^{18),19),39)} which can reasonably well be fitted by NN-exchange models in all compounds discussed in this section.

In order to underline a difference between the spin exchange, described by a conventional Heisenberg interaction, and that in the orbital sector, we consider first the orbital-only models, and move then to the mechanisms which operate in the case of full spin-orbital Hamiltonians with different orbital symmetry and spin values.

3.1. Orbital-exchange, e_g symmetry

On the cubic lattice, the exchange of e_g orbital quantum numbers is described by the Hamiltonian

$$H_{orb} = \frac{2t^2}{U} \sum_{\langle ij \rangle} \tau_i^{(\gamma)} \tau_j^{(\gamma)}, \quad (3.1)$$

where the pseudospin operators $2\tau^{(\gamma)} = \cos\phi^{(\gamma)}\sigma_i^z + \sin\phi^{(\gamma)}\sigma_i^x$ have already been used in Eq. (2.5). Here, the orientation of the bond $\langle ij \rangle$ is specified by the angle $\phi^{(\gamma)} = 2\pi n/3$ with $n = 1, 2, 3$ for $\gamma = a, b, c$ directions, respectively. (For the formal derivation of H_{orb} , consider a spin-polarized version of Eq. (2.5) and set $\vec{S}_i \cdot \vec{S}_j = 4$.)

As pseudospins in Eq. (3.1) interact antiferromagnetically for all bonds, a staggered orbital ordered state is expected to be the ground state of the system. However, linear spin-wave theory, when applied to this Hamiltonian, leads to a gapless two-dimensional excitation spectrum.⁴⁴⁾ This results in an apparent instability of the ordered state at any finite temperature, an outcome that sounds at least counterintuitive. Actually, the problem is even more severe: by close inspection of the orbiton-orbiton interaction corrections, we found that the orbiton self-energy diverges even at zero temperature, manifesting that the linear spin-wave expansion about a classical staggered orbital, Néel-like state *is not adequate* at all.

The origin of these problems is as follows:⁸⁾ By symmetry, there are only a finite number of directions, one of which will be selected as a principal axis for the quadrupole moment. Since this breaks only discrete symmetry, the excitations about the ordered state must have a gap. A linear spin wave theory fails however to give the gap, because Eq. (3.1) acquires a rotational symmetry in the limit of classical orbitals. This results in an infinite degeneracy of classical states, and an *accidental* pseudo-Goldstone mode appears, which is however not a symmetry property of the original *quantum* model (3.1). This artificial gapless mode leads to low-energy divergencies that arise because the coupling constant for the interaction between orbitons does not vanish in the zero momentum limit, as it would happen for a true Goldstone mode. Hence the interaction effects are non-perturbative.

At this point the order-from-disorder mechanism⁴⁵⁾ comes into play: a particular classical state is selected so that the fluctuations about this state maximize the quantum energy gain, and a finite gap in the excitation spectra opens, because in the ground state of the system the rotational invariance is broken. To explore this point explicitly, we calculate quantum corrections to the ground state energy as a function of the angle θ between c -axis and the moment direction. Assuming the latter is perpendicular to b -axis, we rotate globally a pseudospin quantization axes as $\sigma^z \rightarrow \sigma^z \cos\theta - \sigma^x \sin\theta$, $\sigma^x \rightarrow \sigma^x \cos\theta + \sigma^z \sin\theta$, and perform then orbital-wave expansion $\sigma_i^z = 1 - 2a_i^\dagger a_i$, $\sigma_i^x \simeq a_i + a_i^\dagger$ around the classical Néel state, where the staggered moment is now oriented along the new z direction. As a rotation of the quantization axes changes the form of the Hamiltonian, one observes that the magnon excitation spectrum has an explicit θ -dependence:

$$\omega_{\mathbf{p}}(\theta) = 2A \left[1 - \gamma_{\mathbf{p}} - \frac{1}{\sqrt{3}} \eta_{\mathbf{p}} \sin 2\theta - \lambda_{\mathbf{p}} (1 - \cos 2\theta) \right]^{1/2}. \quad (3.2)$$

Here, $\gamma_{\mathbf{p}} = (c_x + c_y)/2$, $\eta_{\mathbf{p}} = (c_x - c_y)/2$, $\lambda_{\mathbf{p}} = (2c_z - c_x - c_y)/6$, and $c_\alpha = \cos p_\alpha$; the energy scale $A = 3t^2/2U$. Calculating the zero point magnon energy $E(\theta) = -\sum_{\mathbf{p}}(A - \frac{1}{2}\omega_{\mathbf{p}}(\theta))$, one obtains an effective potential for the staggered moment direction (three minima at $\theta = \phi^{(\gamma)} = 2\pi n/3$), which at small θ reads as a harmonic one: $E(\theta) = \text{const} + \frac{1}{2}K_{eff}\theta^2$, with an effective ‘‘spring’’ constant $K_{eff} = A\kappa$. The parameter κ is given by

$$\kappa = \frac{1}{3} \sum_{\mathbf{p}} \left[\frac{2\gamma_{\mathbf{p}}}{(1 - \gamma_{\mathbf{p}})^{1/2}} - \frac{\eta_{\mathbf{p}}^2}{(1 - \gamma_{\mathbf{p}})^{3/2}} \right] \approx 0.117. \quad (3.3)$$

The physical meaning of the above calculation is that zero point quantum fluctuations, generated by interactions between spin waves, are enhanced when the staggered moment stays about a symmetric position (one of three cubic axes), and this leads to the formation of the energy profile of cubic symmetry. A breaking of this discrete symmetry results then in the magnon gap, which should be about $\sqrt{K_{eff}/M}$ in the harmonic approximation, where an ‘‘effective inverse mass’’ $1/M$ is of the order of the value of the magnon bandwidth $W = 2\sqrt{2}A$. More quantitatively, the potential $E(\theta)$ can be associated with an effective uniaxial anisotropy term, $\frac{1}{2}K_{eff} \sum_{\langle ij \rangle_c} \sigma_i^z \sigma_j^z$, generated by spinwave interactions in the symmetry broken phase. This low energy effective anisotropy leads to the gap $\Delta = 2\sqrt{AK_{eff}} = 2A\sqrt{\kappa} \sim 0.7A$, stabilizing a long-range ordering. The excitation gap compares to the full magnon bandwidth as $\Delta/W \simeq 0.24$. Almost the same gap/bandwidth ratio for the model (3.1) was also obtained in Ref. 46) by using a different method, i.e. the equation of motion.

The above simple example illustrates a generic feature of orbital-exchange models: The interactions on different bonds are competing (like in the three-state Potts model), and, very different from the Heisenberg-like spin interactions, quantum effects are of crucial importance even for three-dimensional cubic system. In fact, the model (3.1) has a finite classical gap and hence no much dynamics in 2D, thus fluctuations are *more important* in 3D. In this way, the orbital degeneracy provides a new root to frustrated quantum models in three dimensions, in addition to the conventional one driven by geometrical frustration.

It should be interesting to consider the model (3.1) for higher dimensional hypercubic lattices, letting the angle be $\phi^{(\gamma)} = 2\pi n/d$, $n = 1, \dots, d$. With increasing the number of bonds $\gamma = 1, \dots, d$ the energy potential (having d -minima as function of the moment direction θ) will gradually flatten, and hence the gap will eventually close in the limit of infinite dimensions. The ground state and excitations in that limit should be very peculiar.

Finally, by considering a spin-paramagnetic case $\vec{S}_i \cdot \vec{S}_j = 0$ in Eq. (2.5), one would arrive again at the orbital model (3.1), which leads to the G -type staggered order, different from what is seen in manganites well above T_N . Moreover, spin-bond fluctuations in the paramagnetic phase would wash out the three-minima potential, hence preventing the orbital order. This indicates again that the orbital transition at ~ 800 K in LaMnO_3 is primarily not caused by the electronic superexchange.

3.2. Orbital-exchange, t_{2g} symmetry: $YTiO_3$

Now, we discuss the t_{2g} -counterpart of the model (3.1), which shows a more rich behavior. This is because of the higher, threefold degeneracy, and different hopping geometry of a planar-type t_{2g} orbitals that brings new symmetry elements. The orbital order and fluctuations in t_{2g} orbital-exchange model have been studied in Refs. 21) and 22) in the context of ferromagnetic $YTiO_3$. The model reads (in two equivalent forms) as:

$$H_{orb} = \frac{4t^2}{E_1} \sum_{\langle ij \rangle} \left(\vec{\tau}_i \cdot \vec{\tau}_j + \frac{1}{4} n_i n_j \right)^{(\gamma)} \quad (3.4)$$

$$= \frac{2t^2}{E_1} \sum_{\langle ij \rangle} (n_{i\alpha} n_{j\alpha} + n_{i\beta} n_{j\beta} + \alpha_i^\dagger \beta_i \beta_j^\dagger \alpha_j + \beta_i^\dagger \alpha_i \alpha_j^\dagger \beta_j)^{(\gamma)}. \quad (3.5)$$

This is obtained from Eq. (3.11) below by setting $\vec{S}_i \cdot \vec{S}_j = 1/4$ (and dropping a constant energy shift). The energy $E_1 = U - 3J_H$ corresponds to the high-spin virtual transition in the spin-polarized state of $YTiO_3$. In above equations, $\alpha \neq \beta$ specify the two orbitals active on a given bond direction γ (see Fig. 1). For each $(\alpha\beta)^{(\gamma)}$ -doublet, the Heisenberg-like pseudospin $\vec{\tau}^{(\gamma)}$: $\tau_z^{(\gamma)} = (n_\alpha - n_\beta)/2$, $\tau_+^{(\gamma)} = \alpha^\dagger \beta$, $\tau_-^{(\gamma)} = \beta^\dagger \alpha$, and density $n^{(\gamma)} = n_\alpha + n_\beta$ are introduced.

New symmetry elements mentioned above are: (i) a pseudospin interactions are of the Heisenberg form; thus, the orbital doublets like to form singlets just like spins

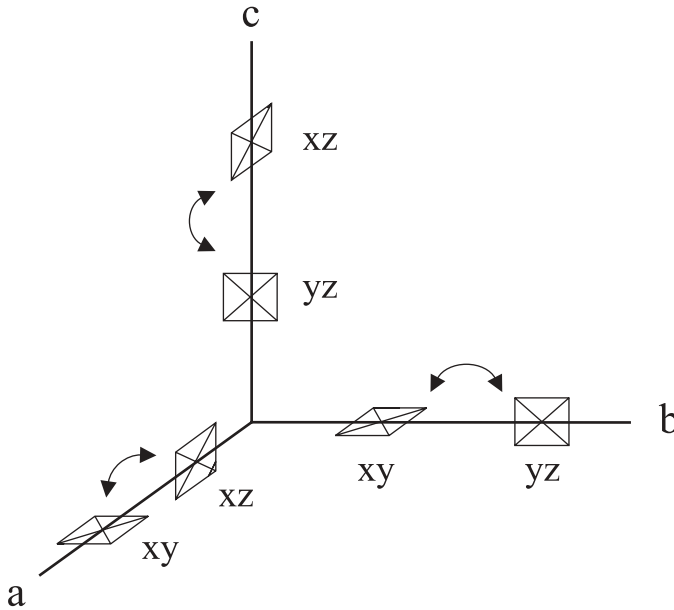


Fig. 1. For every bond of the cubic crystal, two out of three t_{2g} orbitals are equally involved in the superexchange and may resonate. The same two orbitals select also a particular component of angular momentum. (After Ref. 8.)

do. (ii) Apart from an obvious discrete cubic symmetry, the electron density on *each* orbital band is a conserved quantity. Formally, these conservation rules are reflected by a possibility of uniform phase transformation of orbiton operators, that is, $\alpha \rightarrow \alpha \exp(i\phi_\alpha)$, which leaves the Hamiltonian invariant. Moreover, as t_{2g} -orbitals can hop only along two directions (say, xy -orbital motion is restricted to ab planes), the orbital number is conserved on each plane separately.

The above features make the ground state selection far more complicated than in case of e_g -orbitals, as it has in fact been indicated long ago.⁴⁷⁾ In short (see for the technical details Ref. 22)), the breaking of a discrete (cubic) symmetry is obtained via the order-from-disorder scenario again. It turns out, however, that in this case quantum fluctuations select the body diagonals of the cube as a principal axes for the emerging quadrupole order parameter (see Fig. 2). The ordered pattern has a four-sublattice structure, and the density distribution for the first sublattice (with [111] as a principal axis) is described by a function:

$$\rho_1(\vec{r}) = \frac{1}{3}(d_{yz}^2 + d_{xz}^2 + d_{xy}^2) + \frac{2}{3}Q(d_{yz}d_{xz} + d_{yz}d_{xy} + d_{xz}d_{xy}) . \quad (3.6)$$

(Similar expressions can easily be obtained for other sublattices by a proper rotation of the quantization axes according to Fig. 2.) Because of quantum fluctuations, the quadrupole moment Q , which controls the degree of orbital elongation, is anomalously small: $Q \simeq 0.19$ (classically, $Q = 1$).

Surprisingly, not only quadrupole but also a magnetic ordering is equally good for the t_{2g} orbital model. This corresponds to a condensation of complex orbitals giving a finite angular momentum, which is again small, $m_l \simeq 0.19\mu_B$. A magnetic

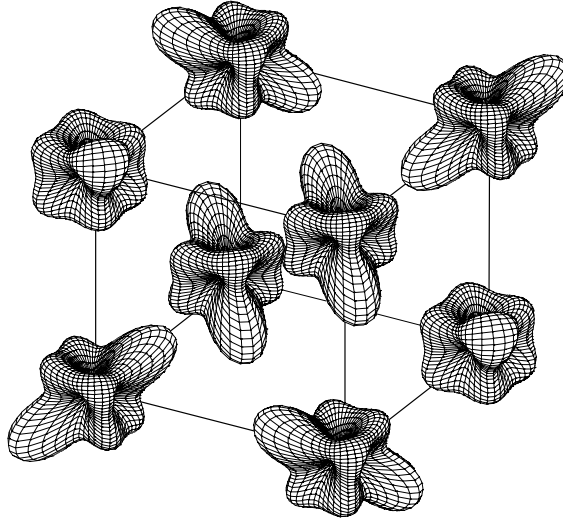


Fig. 2. t_{2g} -electron density in the quadrupole ordered state, calculated from Eq. (3.6). (After Ref. 21).)

pattern is of similar four-sublattice structure. Further, it turns out that quadrupole and magnetic orderings can in fact be continuously transformed to each other — using a phase freedom present in the ground state — and a mixed states do appear in between. We found that these phase degrees of freedom are the gapless Goldstone modes, reflecting the “orbital color” conservation rules discussed above.

On the technical side, all these features are best captured by a radial gauge formalism, applied to the orbital problem in Ref. 22). Within this approach, we represent the orbiton operators, entering in Eq. (3·5), as $\alpha_i = \sqrt{\rho_{i\alpha}} e^{i\theta_{i\alpha}}$, thus separating a density and phase fluctuations. As a great advantage, this makes it possible to single out the amplitude fluctuations (of the short-range order parameters Q , m_l), responsible for discrete symmetry breaking, from a gapless phase-modes which take care of the conservation rules. This way, the ground state *condensate* wave-function was obtained as

$$\psi_{1,2,3,4}(\theta, \varphi) = \sqrt{\rho_0} \left\{ d_{yz} e^{i(\varphi+\theta)} \pm d_{zx} e^{i(\varphi-\theta)} \pm d_{xy} \right\}. \quad (3\cdot7)$$

Here, $\rho_0 \ll 1$ determines the amplitude of the local order parameter, while the phases φ, θ fix its physical nature — whether it is of quadrupole or magnetic type. Specifically, quadrupole and magnetic orderings are obtained when $\varphi = \theta = 0$, and $\varphi = \pi$, $\theta = \pi/3$, respectively. While short-range orbital ordering (a condensate fraction ρ_0) is well established at finite temperature via the order-from-disorder mechanism, true long-range order (a phase-fixing) sets in at zero temperature only. Slow space-time fluctuations of the phases φ, θ are manifested in a 2D gapless nature of the orbital excitations.

In Eq. (3·7), we recognize the “orbital-angle” picture but, because the order parameters are weak ($\rho_0 = Q/3 \sim 0.06$), it represents only a small coherent fraction of the wave function; the main spectral weight of fluctuating orbitals is contained in a many-body wavefunction that cannot be represented in such a simple classical form at all.

The *low-energy* behavior of the model is changed once perturbations from lattice distortions are included. An important effect is the deviation of the bond angles from 180° of an ideal perovskite; this relaxes the orbital-color conservation rules, making a weak orbital order possible at finite temperature. Physically, however, this temperature is confined to the spin ordering, since the interactions as shown in Eq. (3·5) are formed only after the spins get fully polarized, while fluctuating spins destroy the orbital order which is so fragile even in the ground state.

A remarkable feature of the SE driven orbital order is that, although cubic symmetry is locally lifted by a small quadrupole moment, the *bonds* remain perfectly the same, as evident from Fig. 2. This immediately explains a cubic symmetry of the spin-exchange couplings,¹⁹⁾ and of the Raman light scattering from orbital fluctuations,³⁵⁾ — the observations which seem so unusual within a crystal-field picture for $YTiO_3$. This indicates a dominant role of the superexchange mechanism in titanates.

Orbital excitations in $YTiO_3$. — The superexchange theory predicts the follow-

ing orbital excitation spectrum for YTiO_3 :²²⁾

$$\omega_{\pm}(\mathbf{p}) = W_{orb} \left\{ 1 - (1 - 2\varepsilon)(1 - 2f)(\gamma_1 \pm \kappa)^2 - 2(\varepsilon - f)(\gamma_1 \pm \kappa) \right\}^{1/2}, \quad (3.8)$$

where subscript (\pm) indicates two orbiton branches, $\kappa^2 = \gamma_2^2 + \gamma_3^2$, and $\gamma_{1,2,3}$ are the momentum dependent form-factors $\gamma_1(\mathbf{p}) = (c_x + c_y + c_z)/3$, $\gamma_2(\mathbf{p}) = \sqrt{3}(c_y - c_x)/6$, $\gamma_3(\mathbf{p}) = (2c_z - c_x - c_y)/6$ with $c_\alpha = \cos p_\alpha$. Physically, the parameter $\varepsilon \simeq 0.2$ accounts for the many-body corrections stemming from the interactions between orbital waves, which stabilize a weak orbital order via the order-from-disorder mechanism. While the correction $f \sim 0.1$ determines the orbital gap: it would be zero within the model (3.5) itself, but becomes finite once the orbital-nondiagonal hoppings (induced by octahedron tilting in GdFeO_3 -type structure) are included in the calculations. Finally, the parameter $W_{orb} \simeq 2(4t^2/E_1)$ represents an overall energy scale for the orbital fluctuations. By fitting the spin-wave data, $4t^2/E_1 \simeq 60$ meV has been estimated for YTiO_3 in Ref. 22); accordingly, $W_{orb} \sim 120$ meV follows.

The energy scale $4t^2/E_1 \simeq 60$ meV is in fact suggested also by a simple estimation, consider e.g. $t \sim 0.2$ eV and $E_1 \leq 2.5$ eV inferred from optics.⁴⁸⁾ However, it would be a good idea to “measure” this energy from optical experiments, as done for manganites.¹¹⁾ At low temperature, when a spin “filtering factor” ($\vec{S}_i \cdot \vec{S}_j + 3/4$) is saturated for the high-spin transition — see first line in Eq. (3.11) — the ground state energy (per bond) is:

$$\frac{4t^2}{E_1} \left[\left\langle \vec{\tau}_i \cdot \vec{\tau}_j + \frac{1}{4} n_i n_j \right\rangle^{(\gamma)} - \frac{1}{3} \right] = -\frac{4t^2}{3E_1} (|E_0| + 1), \quad (3.9)$$

consisting of a quantum energy $E_0 \simeq -0.214$ (per site) calculated in Ref. 22), and a constant stemming from a linear terms $n_i^{(\gamma)}$ in Eq. (3.11). Using now Eq. (2.8), we find that $K_1 \simeq 0.81 \times (4t^2/E_1)$, which can directly be determined from the optical carrier number $N_{eff,1}$ once measured.

Orbital fluctuations in Raman light scattering. — The superexchange energy for orbital fluctuations, $W_{orb} \sim 120$ meV, is apparently consistent with the energy of a weak signal in the optical transmission data of Ref. 49). Namely, our interpretation, based on *two-orbiton* absorption (similar to the *two-magnon peak* in spin systems), gives $2W_{orb} \sim 240$ meV for the peak position (without a phonon assisting the process), as observed. The same characteristic energy follows also for the Raman scattering,³⁵⁾ which is derived from a two-orbiton propagator with proper matrix elements. However, the most crucial test is provided by a symmetry of the orbital states, controlling the polarization dependences. The superexchange theory outlined above predicts a *broad* Raman band (due to a many-body interactions between the orbital excitations), with the polarization rules of cubic symmetry. Our superexchange-Raman theory is conceptually identical to that for the light scattering on spin fluctuations, and, in fact, the observed orbital-Raman lineshapes are very similar to those of spin-Raman response in cuprates. On the contrary, we found, following the calculations of Ref. 50), that the polarization rules for the *lattice driven* orbital states (2.10) in YTiO_3 strongly disagree with cubic symmetry: The energy positions are completely different for the *c*-axis and *ab* plane polarizations. Such a

strong anisotropy is imposed by a “broken” symmetry of the lattice: in a crystal-field picture, the orbital state is “designed” to fit these distortions (by tuning the orbital-angles).

Comparing the above two models, Eqs. (3·1) and (3·4), we see completely different low-energy behavior — while a finite temperature long-range order is protected by a gap in former case, no gap is obtained for the t_{2g} orbitals. Physically, this is related to the fact that t_{2g} triplet accommodates not only the electric quadrupole moment but — different from e_g doublet — also a true magnetic moment which is a vector like spin. It is this dual nature of the t_{2g} triplet — a Potts-like quadrupole *and* Heisenberg-like vector — which lies at the origin of rich physics of the model (3·4).

3.3. e_g spin-orbital model, spin one-half

Let us move now to the spin-orbital models that describe a simultaneous exchange of both spin and orbital quantum numbers of electrons. We start with the SE model for e_g holes as in perovskites like KCuF_3 , neglecting the Hund’s rule corrections for simplicity. On a three-dimensional cubic lattice it takes the form:⁶⁾

$$H = J \sum_{\langle ij \rangle} \left(\vec{S}_i \cdot \vec{S}_j + \frac{1}{4} \right) \left(\frac{1}{2} - \tau_i \right)^{(\gamma)} \left(\frac{1}{2} - \tau_j \right)^{(\gamma)}, \quad (3\cdot10)$$

where $J = 4t^2/U$, and $\tau^{(\gamma)}$ are the e_g -pseudospins defined above. The main feature of this model — suggested by the very form of Hamiltonian (3·10) — is the strong interplay between spin and orbital degrees of freedom. It was first recognized in Ref. 51), that this simple model contains rather nontrivial physics: the classical Néel state is infinitely degenerate in the orbital sector thus frustrating orbital order and *vice versa*; this extra degeneracy must be lifted by some mechanism (identified later-on in Ref. 52)).

We first notice that the effective spin-exchange constant in this model is definite positive for any configuration of orbitals (as $\tau \leq 1/2$), where its value can vary from zero to J , depending on the orientation of orbital pseudospins. We therefore expect a simple two-sublattice antiferromagnetic, G-type, spin order. There is however a problem: a classical G-type ordering has cubic symmetry and can therefore not lift the orbital degeneracy. In more formal terms, the spin part $(\vec{S}_i \cdot \vec{S}_j + 1/4)$ of the Hamiltonian (3·10) simply becomes zero in this state for all bonds, so that these orbitals effectively do not interact — they are completely uncorrelated. In other words, we gain no energy from the orbital interactions. This shows that from the point of view of the orbitals the classical Néel state is energetically a very poor.

The mechanism for developing intersite orbital correlations (and hence to gain energy from orbital ordering) must involve a strong deviation in the spin configuration from the Néel state — a deviation from $\langle \vec{S}_i \cdot \vec{S}_j \rangle = -\frac{1}{4}$. This implies an intrinsic tendency of the system to develop low-dimensional spin fluctuations which can most effectively be realized by an ordering of elongated $3z^2 - r^2$ orbitals [that is, $\alpha_i = 0$ in Eq. (2·1)]. In this situation the effective spin interaction is *quasi one-dimensional*, so that spin fluctuations are enhanced as much as possible and large quantum energy

is gained from the bonds along the $3z^2 - r^2$ orbital chains. Since $\langle \vec{S}_i \cdot \vec{S}_j + \frac{1}{4} \rangle_c < 0$, the effective orbital-exchange constant that follows from Eq. (3.10) is indeed ferromagnetic, thus supporting $3z^2 - r^2$ type uniform order. At the same time the cubic symmetry is explicitly broken, as fluctuations of spin bonds are different in different directions. This leads to a finite splitting of e_g -levels, and therefore an orbital gap is generated. One can say that in order to stabilize the ground state, a quadrupole order and anisotropic spin fluctuations support and enhance each other — one recognizes here the order-from-disorder phenomenon again.

More quantitatively, the expectation value of the spin-exchange coupling along the c -axis, given by strong $3z^2 - r^2$ orbital overlap [consider $\tau^{(c)} = -1/2$ in Eq. (3.10)], is $J_c = J$, while it is only small in the ab -plane: $J_{ab} = J/16$. Exchange energy is mainly accumulated in c -chains and can be approximated as $J_c \langle \vec{S}_i \cdot \vec{S}_j + \frac{1}{4} \rangle_c + 2J_{ab} \langle \vec{S}_i \cdot \vec{S}_j + \frac{1}{4} \rangle_{ab} \simeq -0.16J$ per site (using $\langle \vec{S}_i \cdot \vec{S}_j \rangle_c = 1/4 - \ln 2$ for 1D and assuming $\langle \vec{S}_i \cdot \vec{S}_j \rangle_{ab} \sim 0$). On the other hand, $x^2 - y^2$ orbital ordering results in the two-dimensional magnetic structure ($J_{a,b} = 9J/16, J_c = 0$) with a much smaller energy gain $\simeq -0.09J$.

From the technical point of view, it is obvious that a conventional expansion around the classical Néel state would fail to remove the orbital degeneracy: Only quantum spin fluctuations can lead to orbital correlations. This is precisely the reason why one does not obtain an orbital gap in a linear spin-wave approximation, and low-energy singularities appear in the calculations,⁵¹⁾ leading to an *apparent* collapse of the spin and orbital order. However, as demonstrated in Ref. 52), the long-range orderings are *stable* against fluctuations, and no “quantum melting” does in fact occur. The singularities vanish once quantum spin fluctuations are explicitly taken into account in the calculations of the orbiton spectrum. These fluctuations generate a finite gap (of the order of $J/4$) for a single orbital as well as for any composite spin-orbital excitation. The orbital gap removes the low-energy divergencies, protecting the long-range spin order. However, spin order parameter is strongly reduced to $\langle S^z \rangle \simeq 0.2$, due to the quasi-one dimensional structure of spin-orbital correlations. Such a spin reduction is generic to spin-orbital models and occurs also in the t_{2g} case, but the mechanism is quite different, as we see below.

Physically, because of the strong spatial anisotropy of the e_g -orbitals, it is impossible to optimize the interactions in all the bonds simultaneously; this results in orbital frustration. The frustration is removed here by reducing the effective dimensionality of the interactions, specifying strong and weak bonds in the lattice. (We may speak of the “Peierls effect” without the phonons; this is essentially what happens in vanadates, too, see later.) At the same time tunneling between different orbital configurations is suppressed: the spin fluctuations produce an energy gap for the rotation of orbitals. A similar mechanism of resolving the frustrations by using the orbital degrees of freedom has recently been discussed in Ref. 53) for vanadium spinels.

Our last point concerns the temperature scales, T_{orb} and T_N . They are in fact *both* controlled by the same energy, that is the orbital gap $\Delta \sim J/4$.⁵²⁾ Once the quadrupole order is lost at $T_{orb} \sim \Delta$ due to the flat 2D orbital modes, spin order

will also collapse. Alternatively, thermal destruction of the spin correlations washes out the orbital gap. Thus, $T_{orb} \sim T_N \sim \Delta$ in the e_g exchange-model alone. [To obtain $T_{orb} \gg T_N$ as commonly observed in e_g compounds experimentally, the orbital frustration should be eliminated by lattice distortions.] In t_{2g} systems, however, a “delay” of T_{orb} , and even $T_{orb} \ll T_N$, is possible. This is because the t_{2g} orbitals are far more frustrated than the Heisenberg spins are. Such an extreme case is in order to be analyzed now.

3.4. t_{2g} spin-orbital model, spin one-half: LaTiO_3

We consider first a full structure of the SE Hamiltonian in titanates. Virtual charge fluctuation spectra for the Ti-Ti pair is represented by a high-spin transition at $E_1 = U - 3J_H$ and low-spin ones at energies $E_2 = U - J_H$ and $E_3 = U + 2J_H$. Here, $U = A + 4B + 3C$ and $J_H = 3B + C$ are the intraorbital repulsion and Hund’s coupling in the Ti^{2+} excited state, respectively.¹⁰⁾ From the optical data of Ref. 48), one may infer that these transitions are located within the energy range from ~ 1 eV to ~ 4 eV. Because of the small spin value, the Hund’s splittings are apparently less than the linewidth, thus these transitions strongly overlap in optics. Indeed, the free-ion value $J_H \simeq 0.59$ eV¹⁰⁾ for Ti^{2+} gives $E_2 - E_1 \simeq 1.2$ eV, compared with a t_{2g} bandwidth ~ 2 eV. (We believe that J_H is further screened in the crystal, just like in manganites¹¹⁾.) Experimentally, the temperature dependence of the optical absorption may help to resolve the transition energies, and to fix thereby the values of U and J_H in crystal. For YTiO_3 , we expect that the E_1 -band should increase (at the expense of the low-spin ones) as the sample is cooled down developing ferromagnetic correlations. The situation in AF LaTiO_3 is, however, much more delicate because of strong quantum nature of spins in this material (recall that the spin-order parameter is anomalously small), and because of the absence of a cooperative orbital phase transition. Thus, we expect no sizable thermal effects on the spectral weight distribution within the $d_i d_j$ -optical multiplet in LaTiO_3 . (Optical response theory for LaTiO_3 , where the quantum effects are of vital importance, is still lacking.) This is in sharp contrast to manganites, where the classical spin- and orbital-orderings lead to a dramatic spectral weight transfer at T_N and T_{str} .¹¹⁾

The above charge fluctuations lead to the SE Hamiltonian^{8), 22)} which we represent in the following form:

$$\begin{aligned}
 H = & \frac{2t^2}{E_1} \left(\vec{S}_i \cdot \vec{S}_j + \frac{3}{4} \right) \left(A_{ij}^{(\gamma)} - \frac{1}{2} n_i^{(\gamma)} - \frac{1}{2} n_j^{(\gamma)} \right) \\
 & + \frac{2t^2}{E_2} \left(\vec{S}_i \cdot \vec{S}_j - \frac{1}{4} \right) \left(A_{ij}^{(\gamma)} + \frac{1}{2} n_i^{(\gamma)} + \frac{1}{2} n_j^{(\gamma)} \right) \\
 & + \left(\frac{2t^2}{E_3} - \frac{2t^2}{E_2} \right) \left(\vec{S}_i \cdot \vec{S}_j - \frac{1}{4} \right) \frac{2}{3} B_{ij}^{(\gamma)}. \quad (3.11)
 \end{aligned}$$

The spin-exchange constants (which determine the magnon spectra) are given by a quantum-mechanical average of the following operator:

$$\hat{J}_{ij}^{(\gamma)} = J \left[\frac{1}{2} (r_1 + r_2) A_{ij}^{(\gamma)} - \frac{1}{3} (r_2 - r_3) B_{ij}^{(\gamma)} - \frac{1}{4} (r_1 - r_2) (n_i + n_j)^{(\gamma)} \right], \quad (3.12)$$

where $J = 4t^2/U$. The parameters $r_n = U/E_n$ take care of the J_H -multiplet splitting, and $r_n = 1$ in the limit of $J_H = 0$. One should note that the spin-exchange constant is *only a fraction* of the full energy scale, represented by J , because of the compensation between contributions of different charge excitations E_n . This is typical when orbital degeneracy is present, but more pronounced for t_{2g} systems where the spin interaction may have either sign even in the $J_H = 0$ limit, see below.

The orbital operators $A_{ij}^{(\gamma)}$, $B_{ij}^{(\gamma)}$ and $n_i^{(\gamma)}$ depend on the bond direction γ , and can be represented in terms of constrained particles a_i, b_i, c_i with $n_{ia} + n_{ib} + n_{ic} = 1$ corresponding to t_{2g} levels of yz, zx, xy symmetry, respectively. Namely,

$$\begin{aligned} A_{ij}^{(c)} &= n_{ia}n_{ja} + n_{ib}n_{jb} + a_i^\dagger b_i b_j^\dagger a_j + b_i^\dagger a_i a_j^\dagger b_j, \\ B_{ij}^{(c)} &= n_{ia}n_{ja} + n_{ib}n_{jb} + a_i^\dagger b_i a_j^\dagger b_j + b_i^\dagger a_i b_j^\dagger a_j, \end{aligned} \quad (3.13)$$

and $n_i^{(c)} = n_{ia} + n_{ib}$, for the pair along the c -axis. Similar expressions are obtained for the a and b bonds, by replacing (ab) -doublets by (bc) and (ca) pairs, respectively. It is also useful to represent $A_{ij}^{(\gamma)}$ and $B_{ij}^{(\gamma)}$ in terms of pseudospins:

$$A_{ij}^{(\gamma)} = 2 \left(\vec{\tau}_i \cdot \vec{\tau}_j + \frac{1}{4} n_i n_j \right)^{(\gamma)}, \quad B_{ij}^{(\gamma)} = 2 \left(\vec{\tau}_i \otimes \vec{\tau}_j + \frac{1}{4} n_i n_j \right)^{(\gamma)}, \quad (3.14)$$

where $\vec{\tau}_i^{(\gamma)}$ operates on the subspace of the orbital doublet $(\alpha, \beta)^{(\gamma)}$ active on a given γ -bond (as already explained above), while a symbol \otimes denotes a product $\vec{\tau}_i \otimes \vec{\tau}_j = \tau_i^z \tau_j^z + (\tau_i^+ \tau_j^+ + \tau_i^- \tau_j^-)/2$.

At large J_H , the ground state of the Hamiltonian (3.11) is obviously ferromagnetic, imposed by the largest E_1 -term, and the problem reduces to the model (3.4), in which: (i) the orbital wave function is described by Eq. (3.7) but, we recall that this is only a small condensate fraction; (ii) low-energy excitations are the 2D, gapless, two-branch, Goldstone phase-modes. Concerning the spin excitations, we may anticipate some nontrivial things even in a ferromagnetic state. Once a magnon is created, it will couple to the orbital phase modes and *vice versa*. At very large J_H , this coupling is most probably of perturbative character but, as J_H is decreased, a bound states should form between the spin and orbital Goldstone modes. This is because the magnons get softer due to increased contributions of the E_2 and E_3 terms. Evolution of the excitation spectra, and the nature of quantum phase transition(s) with decreasing J_H [at which critical value(s)? of which order?] have not yet been addressed so far at all. Needless to say, the finite temperature behavior should be also nontrivial because of the 2D modes — this view is supported also by Ref. 54).

Looking at the problem from the other endpoint, $J_H = 0, E_n = U$, where the ferromagnetic state is certainly lost, one encounters the following Hamiltonian:

$$H = 2J \sum_{\langle ij \rangle} \left(\vec{S}_i \cdot \vec{S}_j + \frac{1}{4} \right) \left(\vec{\tau}_i \cdot \vec{\tau}_j + \frac{1}{4} n_i n_j \right)^{(\gamma)}. \quad (3.15)$$

(An unessential energy shift, equal to $-J$, is not shown here.) This model best illustrates the complexity of t_{2g} orbital physics in perovskites. Its orbital sector,

even taken alone as in Eq. (3·4), is nearly disordered; now, a fluctuating spin bonds will introduce strong disorder in the orbital sector, “deadly” affecting the orbital-phase modes, and hence the long-range coherence which was already so weak. Vice versa, the orbital fluctuations do a similar job in the spin sector; — thus, the bound states mentioned above and spin-orbital entanglement are at work in full strength now.

A while ago,⁷⁾ we proposed that, in the ground state, the model (3·15): (i) has a weak spin order of G -type which respects a cubic symmetry; (ii) the orbitals are fully disordered. Calculations within the framework of $1/N$ -expansion, supporting this proposal, have been presented in that work. Here, we would like to elaborate more on physical ideas that have led to the orbital-liquid picture.

Obviously, quantum dynamics is crucial to lift a macroscopic degeneracy of classical states in the model (3·15), stemming from an infinite number of the “orbital-color conservation” rules discussed above. Various classical orbital patterns (like a uniform $(xy + yz + zx)/\sqrt{3}$, xy orderings, etc.) leave us with Heisenberg spins alone, and hence give almost no energy gain and are ruled out. Quasi-1D orbital order like in the case of the e_g model (3·10) is impossible because of a planar geometry of the t_{2g} orbitals. Yet, the idea of a (dynamical) lowering of the effective dimensionality is at work here again, but underlying mechanism is radically different from that in e_g case.

The key point is a possibility to form orbital singlets. Consider, say, the exchange pair along the c direction. If both ions are occupied by active orbitals ($n_i^{(c)} = n_j^{(c)} = 1$), one obtains the interaction of the form $2J(\vec{S}_i \cdot \vec{S}_j + 1/4)(\vec{\tau}_i \cdot \vec{\tau}_j + 1/4)$ that shows perfect symmetry between spin and orbital pseudospin. The pair has sixfold degeneracy in the lowest energy state: both *spin-triplet*⊗*orbital-singlet* and *spin-singlet*⊗*orbital-triplet* states gain the same exchange energy equal to $-J/2$. In other words, spin exchange constant may have equally strong ferromagnetic and antiferromagnetic nature depending on the symmetry of the orbital wavefunction. This violates the classical Goodenough-Kanamori rules, in which ferromagnetic spin exchange occurs only at finite Hund’s coupling and hence is smaller by factor of J_H/U . In this respect, t_{2g} superexchange clearly differs from the e_g model (3·10), in which the spin-exchange interaction is positively definite because no orbital singlets can be formed in that case.

When such t_{2g} pairs form 1D chain, one obtains a model which has been investigated under the name $SU(4)$ model.^{55),56)} A large amount of quantum energy ($-0.41J$ per site) is gained in this model due to resonance between the local configurations *spin-triplet*⊗*orbital-singlet* and *spin-singlet*⊗*orbital-triplet*. As a result of this resonance, low-energy excitations are of composite spin-orbital nature. In a cubic lattice, the situation is more complicated, as $SU(4)$ spin-orbital resonance along one direction necessarily frustrates interactions in the remaining two directions which require different orbital pairs (see Fig. 1). Given that $SU(4)$ chain physics so ideally captures the correlations, one is nevertheless tempted to consider a “trial” state: the xy orbital is empty, while xz/yz doublets (together with spins) form $SU(4)$ chains along the c -axis — a kind of spin-orbital nematic, with a pronounced directionality

of the correlations. Accounting for the energy-lost on a “discriminated” (classical) ab plane bonds on a mean-field level ($J/8$ per site), we obtain $E_0 = -0.29J$ for our trial state, which is by far better than any static orbital state, and also better than the ferromagnetic state with fluctuating orbitals ($E_0 = -0.214J^{22}$). Once the xy orbital is suppressed in our trial state, the interchain couplings read as

$$H_{ij}^{(a/b)} = J \left(\vec{S}_i \cdot \vec{S}_j + \frac{1}{4} \right) \left(\frac{1}{2} \pm \tau_i^z \right) \left(\frac{1}{2} \pm \tau_j^z \right), \quad (3.16)$$

where \pm sign refers to a/b bond directions. In the ground state, these couplings may induce a weak ordering (staggered between the chains) in both sectors, which, however, should not affect much the intrachain $SU(4)$ physics, by analogy with $\sim 1D$ spin systems.⁵⁷⁾ (This should be an interesting point to consider.)

An assumption made is that a quadrupole order parameter, $Q = n_a + n_b - 2n_c$, responsible for the chain structure, is stabilized by order-from-disorder as in case of e_g quadrupoles in Eq. (3.10), or as it happens in the *spin-one* model for vanadates (see later). However, the t_{2g} quadrupole is highly quantum object, as we have seen above in the context of $YTiO_3$, and it is hard to imagine that the above structure will survive against the xy orbital intervention, that is, “cutting” the $SU(4)$ chains in small pieces and their orientational disorder. One may therefore think of a liquid of “ $SU(4)$ -quadruplets” (a minimal building block to form a spin-orbital singlet^{55),56)}). This way, one arrives at an intuitive picture of dynamical patterns where the local physics is governed by short-range $SU(4)$ correlations, like in quantum dimer models. As a crude attempt to capture the local $SU(4)$ physics, we applied the $1/N$ -expansion to the model (3.15), introducing a bond-operator of mixed spin-orbital nature. A quadrupole disordered state was found indeed lower in energy ($E_0 \simeq -0.33J$)⁷⁾ than a nematic state just discussed. As a $1/N$ -expansion usually underestimates the correlations, we think that a quadrupole disordered state best optimizes the overall quantum energy of the t_{2g} spin-orbital superexchange. An additional energy profit is due to the involvement of all three orbital flavors — a natural way of improving a quantum energy gain. The nature of orbital excitations is the most fundamental problem. Tentatively, we believe that a pseudogap must be present protecting a liquid state; this has already been indicated in Ref. 7) (as an orbital gap, stemming formally from the pairing effects within $1/N$ -expansion).

An important point is that spins and orbitals in the 3D model (3.15) are not equivalent. In the spin sector, the Heisenberg interactions on different bonds cooperate supporting the spin long-range order (albeit very weak) in the ground state. It is the orbital frustration which brings about an unusual quantum physics in a 3D system. When orbitals are disordered, the expectation value of the spin-exchange constant, given by Eq. (3.12), is of AF sign at small J_H , supporting a weak spin- G order in the ground state, on top of underlying quantum spin-orbital fluctuations. Important to note is that the local $SU(4)$ physics is well compatible with a weak spin staggering. The main ingredient of the theory of Ref. 7) is a local $SU(4)$ resonance, which operates on the scale of J and lifts the orbital degeneracy without symmetry breaking. A remote analogy can be drawn with a dynamical JT physics: — the role of phonons are played here by spin fluctuations, and an entangled $SU(4)$ spin-orbital

motion is a kind of vibronic state but living on the bonds. While orbital-lattice vibronic states are suppressed by classical structural transitions, the orbital-spin $SU(4)$ resonance may survive in a lattice due to quantum nature of spins one-half and orbital frustration, and may lead to the orbital disorder in the 3D lattice — this is the underlying idea.

A weak staggering of spins (while the orbitals are disordered) is due to the spin-orbital asymmetry for the 3D lattice. The Hund's coupling J_H brings about yet another asymmetry between the two sectors, but this is now in favor of spin ferromagnetism. J_H changes a balance between two different (AF and F) spin correlations within a $SU(4)$ resonance, and, eventually, a ferromagnetic state with a weak 3D quadrupole order (Fig. 2) is stabilized. Are there any other phases in between? Our *tentative* answer is “yes”, and the best candidate is the spin-orbital nematic discussed above. This state enjoys a fully developed $SU(4)$ physics along the c direction, supported by orbital quadrupole ordering (xy orbital-selection). The xy orbital gap, induced in such a state by J_H in collaboration with order-from-disorder effect, is still to be quantified theoretically. In this intermediate phase, spin and xz/yz doublet correlations are both AF within the planes (see Eq. (3-16)), but different along the $SU(4)$ chains: more ferro (than AF) for spins, and the other way round in the orbital sector. Thus, we predict an intermediate phase with a *weak* spin- C and orbital- G order parameters. Our overall picture is that of the *three competing phases*: (I) spin-ferro and orbitals as in Fig. 2, stable at large J_H ; (II) spin- C , doublets xz/yz are staggered, xy occupation is less than $1/3$; (III) spin- G /orbital-liquid at small J_H . From the experience in vanadates (see next section), we suspect that a tight competition between these states may occur for realistic J_H values. The first (last) states are the candidates for $YTiO_3$ ($LaTiO_3$); it should be a good idea looking for the intermediate one at compositions or compounds “in between”. Needless to say, that all these three states are highly anomalous (compare with 3D Heisenberg systems), because the classical orderings here are just a secondary effects on top of underlying $SU(4)$ quantum fluctuations (or of pure orbital ones at large J_H).

Physically, J_H -tuning is difficult but can be somewhat mimicked by a variation of the Ti-O-Ti bond angle θ (e.g., by pressure). A deviation of it from 180% gives an additional term in the spin-exchange through the small $t_{2g} - e_g$ overlap as it has been pointed out in Ref. 58). According to Ref. 22), this term supports ferromagnetism *equally in all three* directions (different from Ref. 58)). Thus, such a term: $-J' \vec{S}_i \cdot \vec{S}_j$ with $J' \propto \sin^2 \theta$ 22) does not break a cubic symmetry itself, and hence may perfectly drive the above phase transitions. A pronounced quantum nature of the competing phases (because of *quantum orbitals*) may lead to a “soft” character of transitions, as suggested in Ref. 22). Yet another explanation, based on *classical orbital* description, has been proposed in Ref. 58), predicting the spin- A phase as an intermediate state. Thus, the predictions of a quantum and classical orbital pictures are very different: the spin- C *versus* the spin- A type intermediate state, respectively. This offers a nice opportunity to discriminate between the electronic and lattice mechanisms of lifting the orbital degeneracy in titanates.

Summarizing, the Hamiltonians (3-11) and (3-15) are the big “puzzles”, providing a very interesting playground for theory. In particular, the phase transitions

driven by J_H are very intriguing. Concerning again the relation to the titanites: While the most delicate and interesting low-energy problems are (unfortunately) eliminated by weak perturbations like lattice distortions, the major physics — a local $SU(4)$ resonance — should be still intact in LaTiO_3 . This view provides a *hitherto unique* explanation for: (i) an anomalous spin reduction (due to a quantum magnons involved in the spin-orbital resonance, see Ref. 7)); (ii) the absence of a cooperative structural transition (the orbital liquid has no degeneracy, hence no JT instability at small coupling); (iii) nearly ideal cubic symmetry of the spin and Raman responses in both LaTiO_3 and YTiO_3 (in full accord with our theory). The identification of the predicted intermediate spin- C phase is a challenge for future experiments.

3.5. t_{2g} spin-orbital model, spin one: LaVO_3

In the model for titanites, a quantum nature of spins one-half was essential; to make this point more explicit, we consider now similar model but with the higher spin, $S = 1$. Apart from its direct relevance to pseudocubic vanadates AVO_3 , the model provides yet another interesting mechanism of lifting the degeneracy by SE interactions: here, the formation of the quantum orbital chains is the best solution.³⁸⁾

The interactions between $S = 1$ spins of V^{3+} ions arise from the virtual excitations $d_i^2 d_j^2 \rightarrow d_i^1 d_j^3$, and the hopping t is allowed only between two out of three t_{2g} orbitals, just as in titanites. The d_i^3 excited state may be either (i) a high-spin 4A_2 state, or one of a low-spin ones: (ii) the degenerate 2E and 2T_1 states, or (iii) a 2T_2 level. The excitation energies are $E_1 = U - 3J_H$, $E_2 = U$ and $E_3 = U + 2J_H$, respectively,¹⁰⁾ where $U = A + 4B + 3C$ and $J_H = 3B + C$. For the free ion V^{2+} , one has $J_H \simeq 0.64 \text{ eV}$ ¹⁰⁾ but this should be screened in crystal to $\simeq 0.5 \text{ eV}$ as suggested in Ref. 14). Correspondingly, the SE Hamiltonian consists of three contributions, like in Eq. (3·11), but a different form as obtained in Ref. 38) is more instructive here:

$$H = \sum_{\langle ij \rangle} \left[(\vec{S}_i \cdot \vec{S}_j + 1) \hat{J}_{ij}^{(\gamma)} + \hat{K}_{ij}^{(\gamma)} \right]. \quad (3\cdot17)$$

In terms of operators $A_{ij}^{(\gamma)}$, $B_{ij}^{(\gamma)}$ and $n_i^{(\gamma)}$ introduced previously in Eqs. (3·13) and (3·14), the orbital operators $\hat{J}_{ij}^{(\gamma)}$ and $\hat{K}_{ij}^{(\gamma)}$ read as follows:

$$\hat{J}_{ij}^{(\gamma)} = \frac{J}{4} \left[(1 + 2\eta R) A_{ij}^{(\gamma)} - \eta r B_{ij}^{(\gamma)} - \eta R (n_i + n_j) \right]^{(\gamma)}, \quad (3\cdot18)$$

$$\hat{K}_{ij}^{(\gamma)} = \frac{J}{2} \left[\eta R A_{ij}^{(\gamma)} + \eta r B_{ij}^{(\gamma)} - \frac{1}{2} (1 + \eta R) (n_i + n_j) \right]^{(\gamma)}. \quad (3\cdot19)$$

Here $J = 4t^2/U$, as usual. The coefficients $R = U/E_1 = 1/(1 - 3\eta)$ and $r = U/E_3 = 1/(1 + 2\eta)$ with $\eta = J_H/U$ take care of the J_H -multiplet structure.

If we neglect the Hund's splitting of the excited states (consider $\eta \rightarrow 0$ limit), the Hamiltonian (3·17) reduces to:

$$H = J \sum_{\langle ij \rangle} \frac{1}{2} (\vec{S}_i \cdot \vec{S}_j + 1) \left(\vec{\tau}_i \cdot \vec{\tau}_j + \frac{1}{4} n_i n_j \right)^{(\gamma)}, \quad (3\cdot20)$$

where a constant energy of $-2J$ per site is neglected. This result should be compared with corresponding limit in the d^1 case, Eq. (3.15). One observes different spin structures: $\frac{1}{2}(\vec{S}_i \cdot \vec{S}_j + 1)$ is obtained for vanadium ions instead of $2(\vec{S}_i \cdot \vec{S}_j + \frac{1}{4})$ for spins one-half of Ti^{3+} . The difference in spin values can in fact be accounted for in general form as $(\vec{S}_i \cdot \vec{S}_j + S^2)/2S^2$. It is important also to note that we have two electrons per V^{3+} ion; one therefore has a different constraint equation for orbital densities $n_{ia} + n_{ib} + n_{ic} = 2$.

It is instructive to start again with a single bond along the c -axis. A crucial observation is that the lowest energy of $-J/2$ is obtained when the spins are *ferromagnetic*, and the orbitals a and b form a *singlet*, with $\langle \vec{\tau}_i \cdot \vec{\tau}_j \rangle^{(c)} = -\frac{3}{4}$. *Spin singlet* \otimes *orbital triplet* level is higher (at $-J/4$). This is in sharp contrast to the $S = 1/2$ case, where the *spin singlet* \otimes *orbital triplet* and the *spin triplet* \otimes *orbital singlet* configurations are degenerate, resulting in a strong quantum resonance between them as it happens in titanates. Thus, ferromagnetic interactions are favored due to a local orbital singlet made of a and b orbitals. Dominance of high spin configuration reflects simply the fact that the spin part of the interaction, that is $(\vec{S}_i \cdot \vec{S}_j + S^2)/2S^2$, is equal to 1 for a ferromagnetic configuration, while vanishing in spin-singlet sector (as $-1/S$) in the limit of large spins. In order to form ab -orbital singlet on the bond along c -axis, the condition $n_i^{(c)} = n_j^{(c)} = 1$ must be fulfilled (no $\vec{\tau}^{(c)}$ pseudospin can be formed otherwise). This implies that the second electron on both sites has to go to an inactive (that is xy) orbital. Thus we arrive at the following picture for the superexchange bond in c direction: (i) spins are aligned ferromagnetically, (ii) one electron on each site occupies either a or b orbital forming a $SU(2)$ invariant orbital pseudospins that bind into the orbital singlet, (iii) the xy orbital obtains a stabilization energy of about $-J/2$ (the energy required to break ab -orbital singlet) and accommodates a remaining, second electron.

Formation of one-dimensional orbital chains. — If the high spin state of the given pair is so stable, why does then a whole crystal not form uniform ferromagnet? That is because each site has two electrons, and an orbital that is inactive in particular (ferromagnetic bond) direction, induces in fact an antiferromagnetic coupling in the other two directions. Thus spin interactions are strongly ferromagnetic (supported by orbital singlets) in one direction, while the other bonds are antiferromagnetic. As all directions are *a priori* equivalent in a cubic lattice, we again arrive at the problem of “orbital frustration” common to all spin-orbital models on high-symmetry lattices. The solution of this problem here is as follows. As the spin-orbital resonance like in titanates is suppressed in the present case of large spin $S = 1$, quantum energy can be gained mainly from the orbital sector. This implies that a particular classical spin configuration may be picked up which maximizes the energy gain from orbital fluctuations. Indeed, orbital singlets (with $n_{ia} + n_{ib} = 1$) may form on the bonds parallel to the c -axis, exploiting fully the $SU(2)$ orbital physics in one direction, while the second electron occupies the third t_{2g} orbital ($n_{ic} = 1$), controlling spin interactions in the ab -planes. Thus one arrives at spin order of the C-type [ferromagnetic chains along c -axis which stagger within ab -planes], which best comprises a mixture of ferromagnetic (driven by the orbital singlets) and antiferro-

magnetic (induced by the electron residing on the static orbital) interactions. This is an analogy of the intermediate phase that we introduced for titanites above; here, it is much more stable because of the large spin value.

Once the C-type spin structure and simultaneous selection among the orbitals (fluctuating a, b orbitals, and stable c orbital located at lower energy) is made by spontaneous breaking of the cubic symmetry, the superexchange Hamiltonian can be simplified. We may set now $n_{ic} = 1, n_{ia} + n_{ib} = 1$, and introduce pseudospin $\vec{\tau}$ which operates within the (a, b) orbital doublet exclusively.

We focus first on orbital sector as quantum dynamics of the system is dominated by the orbital pseudospins $\tau = \frac{1}{2}$ rather than by large spins $S = 1$. In the classical C-type spin state, $(\vec{S}_i \cdot \vec{S}_j + 1)$ is equal 2 along the c -direction while it is zero on ab -plane bonds. In this approximation, orbital interactions in the model (3.17) are given by $(2\hat{J}_{ij}^{(c)} + \hat{K}_{ij}^{(c)})$ on c -axis bonds, while on ab -plane bonds only the $\hat{K}_{ij}^{(a,b)}$ term contributes which is *small*. Expressing $A_{ij}^{(\gamma)}$ and $B_{ij}^{(\gamma)}$ operators in Eqs. (3.18) and (3.19) via pseudospins $\vec{\tau}$, one arrives at the following orbital Hamiltonian:³⁸⁾

$$H_{orb} = J_{orb} \sum_{\langle ij \rangle || c} (\vec{\tau}_i \cdot \vec{\tau}_j) + J_{orb}^{\perp} \sum_{\langle ij \rangle || (a,b)} \tau_i^z \tau_j^z, \quad (3.21)$$

where $J_{orb} = JR$ and $J_{orb}^{\perp} = J\eta(R+r)/2$. As their ratio is small, $J_{orb}^{\perp}/J_{orb} = \eta(1 - 5\eta r/2)$ (that is about only 0.1 for the realistic values of parameter $\eta = J_H/U$ for vanadates), we obtain one-dimensional orbital pseudospin chains coupled only weakly to each other. Orbital excitations in the model (3.21) are mostly propagating along c -chain directions. Their spectrum can be calculated, e.g., within a linear spin-wave approximation, assuming a weak orbital order due to interchain coupling J_{orb}^{\perp} . One indeed obtains the one-dimensional *orbital-wave* spectrum:³⁸⁾

$$\omega_{\mathbf{p}} = \sqrt{\Delta^2 + J_{orb}^2 \sin^2 p_z}, \quad (3.22)$$

which shows the gap $\Delta = J\{\eta(R+r)[2R + \eta(R+r)]\}^{1/2}$ at $p_z = \pi$. The orbital gap Δ is small and grows with increasing Hund's coupling as $\propto J\sqrt{\eta}$.

Alternatively, one can use the Jordan-Wigner fermionic representation to describe quasi one-dimensional orbital dynamics, as suggested in Ref. 14). One obtains the 1D *orbitoron* dispersion:

$$\varepsilon_{\mathbf{k}} = \sqrt{h^2 + J_{orb}^2 \cos^2 k_z}, \quad (3.23)$$

where $h = 4\tau J_{orb}^{\perp}$ is the ordering field stemming from interchain interactions. The staggered orbital order parameter $\tau = |\langle \tau_i^z \rangle|$, determined self-consistently from $\tau = \sum_k (h/2\varepsilon_k) \tanh(\varepsilon_k/2T)$, is small, and orbitals strongly fluctuate even at $T = 0$.

The underlying 1D-orbital dynamics have an important consequences on spin interactions which control spinwave dispersions. In the spin sector, we obtain interactions $J_c(\vec{S}_i \cdot \vec{S}_j)$ and $J_{ab}(\vec{S}_i \cdot \vec{S}_j)$, with the spin-exchange constants following from Eq. (3.18). The result is given by orbital pseudospin correlations:

$$J_c = \frac{J}{2} \left[(1 + 2\eta R) \left\langle \vec{\tau}_i \cdot \vec{\tau}_j + \frac{1}{4} \right\rangle - \eta r \left\langle \vec{\tau}_i \otimes \vec{\tau}_j + \frac{1}{4} \right\rangle - \eta R \right],$$

$$J_{ab} = \frac{J}{4} \left[1 - \eta(R + r) + (1 + 2\eta R - \eta r) \left\langle \vec{\tau}_i \otimes \vec{\tau}_j + \frac{1}{4} \right\rangle \right]. \quad (3.24)$$

While in-plane antiferromagnetic couplings are mostly determined by the classical contribution of xy orbitals (first term in J_{ab}), the exchange constant along the c -axis has substantial quantum contribution represented by the first term in J_c . This contribution is of negative sign due to the orbital singlet correlations along chains. The pseudospin expectation values in Eq. (3.24) can be estimated by using either the Jordan-Wigner fermionic-orbital representation¹⁴⁾ or within orbital-wave approximation.³⁸⁾ In both cases, one observes that the ferromagnetic coupling along the c -axis is strongly enhanced by orbital fluctuations. For a realistic values of $\eta \sim 0.12$, one obtains $-J_c \sim J_{ab} \sim J/5$. This result is qualitatively different from that expected from the Goodenough-Kanamori rules. Indeed, in that classical picture with fully ordered orbitals one would obtain instead the smaller value $-J_c \sim 2\eta R J_{ab} \sim J_{ab}/2$.

Comparing all the coupling constants in both spin and orbital sectors, one observes that Heisenberg-like orbital dynamics has the largest energy scale, $J_{orb} = JR$, thus dominating the physics of the present spin-orbital model. The overall picture is that “cubic frustration” is resolved here by the formation of the orbital chains with Heisenberg dynamics, from which a large quantum energy is gained. This is similar to the order-from-disorder scenario for the e_g spin-orbital model (3.10), where classical $3z^2 - r^2$ orbital order results in quasi one-dimensional spin chains. In the present t_{2g} orbital model with large classical spins, the role of spins and orbitals are just interchanged.

As argued in Ref. 38), the above scenario may explain the C -AF type spin order in LaVO_3 .⁵⁹⁾ A structural transition that follows the onset of magnetic order in this compound is also natural in the superexchange model. Indeed, C -type spin ordering and formation of the pseudospin orbital chains are intimately connected and support each other. Thus, the ordering process in the orbital sector — the stabilization of xy orbital which absorbs one electron, and lifting the remaining degeneracy of xz/yz -doublet via quantum fluctuations — occurs cooperatively with the evolution of the C -type magnetic order. In more formal terms, the classical order parameters $Q_{orb} = (2n_c - n_a - n_b)$ (xy -orbital selection) and $Q_{sp} = (\langle \vec{S}_i \cdot \vec{S}_j \rangle_c - \langle \vec{S}_i \cdot \vec{S}_j \rangle_{ab})/2$ (spin-bond selection) act cooperatively to break the cubic symmetry, while the energetics is driven by a quantum energy released by xz/yz orbital fluctuations. Obviously, this picture would break down *if* the JT-coupling dominates — nothing but a conventional 3D-classical ordering of xz/yz -doublets at some T_{str} , independent of spin correlations, would take place in that case.

A pronounced anisotropy and temperature dependence of the optical conductivity observed in LaVO_3 ⁵⁹⁾ also find a *quantitative* description¹⁴⁾ within this theory, in which quantum orbital fluctuations play the key role. Interestingly, the JT picture has also been applied to the problem, see Ref. 60). Based on first-principle calculations, a JT binding energy $E_{JT} \sim 27$ meV has been obtained. Consequently, a large orbital splitting ($= 4E_{JT}$) suppresses the quantum nature of orbitals and, as a result, one obtains that the optical spectral weights along the c and a, b directions are almost the same, $I_c/I_{ab} \simeq 1$, contradicting the experiment which shows strong

polarization dependence. In our view, the optical experiments⁵⁹⁾ clearly indicate that JT coupling is much smaller than estimated in Ref. 60), and are thus not sufficient to lock-in the orbitals in LaVO₃. At this point, we are faced again with a problem of the principal importance: Why do the first-principle calculations always predict a large orbital splittings? should those numbers be directly used as an input parameters in the many-body Hamiltonians, suppressing thereby all the interesting orbital physics? These questions remain puzzling.

Based on the above theory, and by analogy with titanites, we expect that the Raman light scattering on orbital fluctuations in vanadates should be visible as a *broad* band in the energy range of two-orbion excitations, $2J_{orb}$, of the quantum orbital chains. Given a single-orbion energy scale $J_{orb} = JR \sim 60 - 70$ meV (which follows from the fit of optical⁵⁹⁾ and neutron scattering³⁹⁾ data), we predict a broad Raman band centered near ~ 120 meV. This energy is smaller than in titanites because of the low-dimensionality of orbital dynamics, and falls in the range of two-phonon spectra. However, the orbital-Raman band is expected to have very large width (a large fraction of J_{orb}), as orbitons strongly scatter on spin fluctuations (as well on phonons, of course). More specifically, we observe that both thermal and quantum fluctuations of the spin-bond operator, $(\vec{S}_i \cdot \vec{S}_j + 1)$ in Eq. (3-17) or (3-20), introduce an effective disorder in the orbital sector. In other words, the orbital Hamiltonian (3-21) obtains a strong bond-disorder in its coupling constants, hence the expected incoherence and broadness of the orbital Raman response. This feature, as well as a specific temperature and polarization dependences should be helpful to discriminate two-orbion band from two-phonon (typically, sharply structured) response. On the theory side, the light scattering problem in the full spin-orbital model (3-17) need to be solved in order to figure out the lineshape, temperature dependence, etc. Alternatively, a crystal-field and/or first-principle calculations would be helpful, in order to test further the “lattice-distortion” picture for vanadates, — in that case, the Raman-band frequencies would be dictated by the on-site level structure.

Let us conclude this section, devoted to the spin-orbital models: Orbital frustration is a generic feature of the superexchange interactions in oxides, and leads to a large manifold of competing states. Reduction of the effective dimensionality by the formation of quantum spin- or orbital-chains (depending on which sector is “more quantum”) is one way of resolving the frustrations. In e_g spin-orbital models, the order-from-disorder mechanism completes the job, generating a finite orbital gap below which a classical description becomes valid. In superexchange models for titanites, where both spins and orbitals are of quantum nature, a composite spin-orbital bound states may develop in the ground state, lifting the orbital degeneracy *without breaking* the cubic symmetry. The nature of such a quantum orbital-liquid and its elementary excitations is of great theoretical interest, regardless to which extend it is “spoiled” in real materials. The interplay between the SE interactions, dynamical JT coupling, and extrinsic lattice distortions is a further step towards a quantitative description of the electronic phase selection in titanites.

§4. Competition between superexchange and lattice effects: YVO_3

As an example of the phase control by a competing superexchange, lattice, temperature and doping effects, we consider now a slightly modified version of the $S = 1$ model (3·17) for vanadates, by adding there the following Ising-like term which operates on the bonds along c direction:³⁸⁾

$$H_V = -V \sum_{\langle ij \rangle \| c} \tau_i^z \tau_j^z. \quad (4.1)$$

This describes a ferromagnetic ($V > 0$) orbital coupling, which competes with the orbital-Heisenberg J_{orb} -term in the Hamiltonian (3·21). Physically, this term stands for the effect of GdFeO_3 type distortions including A–O covalency, which prefer a stacking (“ferromagnetic” alignment) of orbitals along c direction.⁶¹⁾ This effect gradually increases as the size of A-site ion decreases and may therefore be particularly important for YVO_3 . Interesting to note that the V -term makes the orbital interactions of xyz -type with z -coupling being smaller, hence driving the orbital sector towards a more disordered xy model limit (motivating the use of Jordan-Wigner representation for orbitals¹⁴⁾). However, when increased above a critical strength, the V -term favors a classically ordered orbitals.

Three competing phases can be identified for the modified, Eqs. (3·17) plus (4·1), model. (i) The first one, which is stable at moderate $V < J$, was that just considered above: C -type spin order with fluctuating orbitals (on top of a very weak staggered order) as in LaVO_3 . This state is driven by a cooperative action of orbital-singlet correlations and J_H -terms. (ii) At large $V > J$, the orbitals order ferromagnetically along the c -axis, enforcing the G -type spin order, as observed in YVO_3 . (iii) Yet there is a third state, which is “hidden” in the SE-model and may become a ground state when both J_H and V are below some critical values. This is a valence bond solid (VBS) state, which is derived by a dimerization of the Heisenberg orbital chains, by using the spin-bond operators $(\vec{S}_i \cdot \vec{S}_j + 1)$ as an “external” dimerization field. (We already mentioned this operator as a “disorder field” for the orbital excitations.)

Specifically, consider the limit of $\eta = 0$, $V = 0$, where we are left with the model (3·20) alone. It is easy to see that we can gain more orbital quantum energy by choosing the following spin structure: On every second c -axis bond, spins are ferromagnetic, $(\vec{S}_i \cdot \vec{S}_j + 1) = 2$, while they are antiparallel in all other bonds giving $(\vec{S}_i \cdot \vec{S}_j + 1) \sim 0$. Consequently, the orbital singlets are fully developed on ferro-spin bonds, gaining quantum energy $-J/2$ and supporting the high-spin state assumed. On the other hand, the orbitals are completely decoupled on AF-spin bonds. As a result, the expectation value $\langle \vec{\tau}_i \cdot \vec{\tau}_j \rangle$ vanishes on these “weak” bonds, thus the spin exchange constant $J_s^{weak} = J/8$ (consider Eq. (3·24) for uncorrelated orbitals and the $\eta = 0$ limit) turns out to be positive, consistent with antiferromagnetic spin alignment on these bonds. Such a self-organized spin-orbital dimer state is lower in energy [$-J/4$ per site] than a uniform Heisenberg orbital chains with C -type spin structure [$(1/2 - \ln 2)J \simeq -0.19J$]. Thus, the VBS state (building blocks are the decoupled orbital dimers with total spin 2) is a competing state at small η values, as has been noticed by several authors.^{62), 39), 40), 63), 64)}

4.1. Phase diagram

Interplay between the above three spin-orbital structures has been investigated numerically in Ref. 64) within the DMRG method. The thermodynamic properties and interesting evolution of correlation functions have also been studied by using the finite-temperature version of DMRG.^{40),39)} Though these methods are restricted to the one-dimensional version of the model, they give rigorous results and are in fact quite well justified, because the essential physics is governed by strong dynamics within the $\sim 1D$ orbital chains, while a weak interchain couplings can be implemented on a classical mean-field level.⁴⁰⁾

The ground state phase diagram in the η - V plane, obtained from the DMRG study⁶⁴⁾ is shown in Fig. 3. There are three distinct phases in this figure. For small η and V , the VBS state is stabilized, which is driven either to the orbital-ferromagnetic/spin-AF phase (called G) with the increase of V , or to the orbital-AF/spin-ferromagnetic one (called C) with the increase of the Hund's coupling η . The critical value $\eta_c(V=0) \simeq 0.11$ for the latter transition perfectly agrees with the earlier result inferred from the finite-temperature DMRG-study,⁴⁰⁾ and is just slightly below the realistic values in vanadates.²⁵⁾ This indicates the proximity of VBS state in vanadates, on which we elaborate later-on. Note that when the Hund's coupling is slightly above the critical value, the ground state is spin-ferromagnetic for small V , but for intermediate values of V the VBS-state is stabilized. Stabilization of the *orbital disordered* state by finite V interaction (induced by *lattice distortion*) is a remarkable result. The physics behind this observation is that — as already mentioned — the interaction (4.1) introduces a frustration into the orbital sector, competing with antiferro-type alignment of orbitals in the SE model.

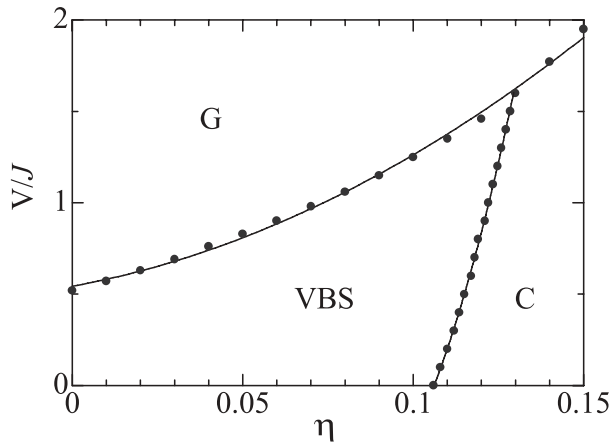


Fig. 3. Phase diagram in the η - V plane. The VBS state consists of orbital-singlet dimers with spin 2, and the spins of different dimers are weakly coupled antiferromagnetically. In the phase C , a uniform orbital-chain is restored, while the spins are aligned ferromagnetically along the chain. The phase G is the spin-AF/orbital-ferromagnetic state, stabilized by the Ising interaction between the orbitals originating from the GdFeO₃-type distortions. All the phase transitions are of first-order. (After Ref. 64.)

The V -driven phase transition from the spin- C to spin- G ground state, obtained in these calculations describes physically why an increased GdFeO_3 -type distortion promotes a spin-staggering along the c direction in YVO_3 , while less distorted LaVO_3 has the spin- C structure. This study also suggests that $V \sim J$ in vanadates. As $J \sim 40$ meV in these compounds,^{39),14)} we suspect that the effect of GdFeO_3 -type distortions on t_{2g} orbitals is roughly of this scale in perovskites in general, including titanites. Being comparable with the SE scale $J_{orb} \sim 60$ meV in vanadates, the V -term is important to stabilize the spin- G phase, but it is not sufficient to lock-in the orbitals in titanates, where *the three dimensional* exchange fluctuations are characterized by larger energies of the order of $W_{orb} \sim 120$ meV (see previous Section).

4.2. Entropy driven spin-orbital dimerization

YVO_3 is a remarkable material, in the sense that its spin- G type ground state is very fragile and readily changes to the spin- C state via the phase transition, driven either by temperature (at 77 K) or by small doping.⁶⁵⁾ This finds a natural explanation within the present theory in terms of competing phases, assuming that YVO_3 is located in the phase G near the tricritical point (see the phase diagram in Fig. 3), and thus close to the spin- C and VBS states.

This view is strongly supported by the neutron scattering data of Ref. 39). This experiment revealed several anomalies, indicating that the spin- C phase above 77 K is itself very unusual: (i) substantial modulations of the spin couplings along the c direction, (ii) ferromagnetic interactions are stronger than ab -plane AF ones, (iii) anomalously small ordered moment, which (iv) selects the ab -plane (different from the easy c -axis found just below 77 K or in the C -phase of LaVO_3). All these features have coherently been explained in Ref. 39) in terms of underlying quantum dynamics of the spin-orbital chains and their *entropy-driven* dimerization.⁴⁰⁾ Physics behind the last point is as follows.

Because the Hund's coupling parameter is close to the critical one, there is strong competition between uniform (C) and dimerized (VBS) states, and this may affect thermodynamic properties for entropy reasons. The point is that the dimer state contains "weak" spin bonds: spin interaction between different dimers is small when η is near the critical value (when the dimerization amplitude is not saturated, weak bonds are ferromagnetic but much weaker than strong ferromagnetic bonds within the dimers). Therefore, the spin entropy of an individual dimer with total spin 2, that is $\ln 5$, is released. The gain of spin entropy due to the dimerization lowers the free energy $F = \langle H \rangle - TS$ and may stabilize a dimerized state with alternating weak and strong ferro-bonds along c -axis. In other words, the dimerization of spin-orbital chains occurs due to the *orbital Peierls effect*, in which thermal fluctuations of the spin bond-operator $(\vec{S}_i \cdot \vec{S}_j)_c$ play the role of lattice degrees of freedom, while the critical behavior of the Heisenberg-like orbital chains is a driving force. As the dimerization is of electronic origin, and is not as complete as in the VBS state itself, concomitant lattice distortions are expected to be small.

These qualitative arguments have been substantiated by numerical studies using the finite-temperature DMRG method.^{40),39)} The explicit calculations of the entropy,

evolution of the dimer correlations upon increasing temperature, and anomalous behavior of spin and orbital susceptibilities can be found in these papers.

4.3. Doping control

The energy difference between G and C type spin orderings in YVO_3 is very small, $E_C - E_G \sim 0.1J \sim 4 \text{ meV}$ only^{38), 64)} for realistic values of η and V . Therefore, the G -type ground state of YVO_3 can easily change to the C -type upon small perturbations. For instance, pressure may reduce the GdFeO_3 distortions hence the V -interaction, triggering the first-order phase transition described above. Injection of the charge carriers is the another possibility, which we discuss now (see also Ref. 66)).

We need to compare a kinetic energy gains in above-mentioned competing phases. It is easy to see that the charge-carriers strongly favor spin- C phase, as they can freely move along the ferromagnetic spin chains in the c direction of the C phase, while a hole-motion is frustrated in the spin- G phase in all directions. In more detail, the ab -plane motion is degraded in both phases equally by a classical AF order via the famous “double-exchange factor” $\cos \frac{\theta}{2}$ with $\theta = \pi$ for antiparallel spins. Thus, let us focus on the c direction. In the G -phase, a hole-motion is disfavored again by antiparallel spins ($\theta_c = \pi$), but the spin- C phase with $\theta_c = 0$ is not “resistive” at all. Now, let us look at the orbital sector. The orbitals are fully aligned in the spin- G phase and thus introduce no frustration. Our crucial observation is that the orbitals are not resistive to the hole motion in the spin- C phase, too. The point is that a doped-hole in the spin- C phase can be regarded as a *fermionic-holon* of the quasi-1D orbital chains, and its motion is not frustrated by orbitals at all. This is because of the orbital-charge separation just like in case of a hole motion in 1D Heisenberg chains.⁶⁷⁾ As a result, the c direction is fully transparent in the spin- C phase (both in spin and orbital sectors), and doped holes gain a kinetic energy $K = 2tx$ per site at small x . (On contrast, a hole motion is strongly disfavored in spin- G phase because of AF-alignment of large spins $S = 1$, as mentioned.) Even for the doping level as small as $x = 0.02$, this gives an energy gain of about 8 meV (at $t \sim 0.2 \text{ eV}$) for the C phase, thus making it *lower* in energy than the G -phase. This is precisely what is observed.⁶⁵⁾ The underlying quantum orbital chains in the spin- C phase³⁸⁾ are of crucial importance here: a *static* configuration of the staggered xz/yz orbitals would discourage a hole-motion. In other words, fluctuating orbitals not only support the ferromagnetic spins, but also well accommodate doped holes because of orbital-charge separation. The *quantum orbitals* and a doping induced *double-exchange* act cooperatively to pick up the spin- C phase as a ground state.

The “holon-like” behavior of the doped-holes implies a quasi one-dimensional charge transport in doped vanadates, namely, a much larger and strongly temperature dependent low-energy optical intensity (within the Mott-gap) along the c -axis, in comparison to that in the ab -plane polarization. The situation would be quite different in case of classical JT orbitals: A staggered 3D-pattern of static orbitals frustrates hole motion in all three directions, and only a moderate anisotropy of the low-energy spectral weights is expected. This way, optical experiments in a doped compounds have a potential to discriminate between the classical JT picture and

quantum orbitals, just like in the case of pure LaVO_3 as discussed above.

The doping-induced transition from the G to the C phase must be of the first order, as the order parameters and excitations of the G phase in both spin and orbital sectors hardly change at such small doping levels. Specifically, AF spin coupling J_c in the G phase may obtain a double-exchange ferromagnetic correction $J_{DE} < K/4S^2 = tx/2$ due to the local vibrations of doped holes, which is about 2 meV only at the critical doping $x \sim 0.02$. This correction is much smaller than $J_c \simeq 6 \text{ meV}$ ³⁹⁾ of undoped YVO_3 . Regarding the orbitals, they are perfectly aligned “ferromagnetically” along the c -axis in the ground state of YVO_3 , satisfying the GdFeO_3 distortion; we find that this is not affected by 1–2% doping at all. Our predictions are then as follows: The staggered spin moment and spinwave dispersions of the G phase remain barely unrenormalized upon doping, until the system suddenly changes its ground state. On the other hand, we expect that doping should lead to sizable changes in the properties of spin- C phase, because of the positive interplay between the “holons” formed and underlying orbital quantum physics. Our predictions are opposite to those of Ref. 66); this gives yet another opportunity to check experimentally (by means of neutron scattering) which approach — SE quantum picture or classical JT orbitals — is more appropriate for the spin- C phase of vanadates.

A more intriguing question is, however, whether the doping induced C -phase of YVO_3 is also dimerized as in the undoped YVO_3 itself, or not. Theoretically, this is well possible at small doping, and, in fact, we expect that the orbital Peierls effect should cooperate with a conventional fermionic one, stemming from the hopping-modulation of doped carriers along the underlying orbital chains.

Summarizing this section, we conclude that the t_{2g} spin-orbital model with high spin values shows an intrinsic tendency towards dimerization. Considered together with lattice induced interactions, this leads to a several low-energy competing many-body states, and to the “fine” phase-selection by temperature, distortions and doping. One of these phases is the spin- G phase with classical orbitals; it is well isolated in the Hilbert space and hence may show up only via a discontinuous transition.

§5. Lifting the orbital degeneracy by spin-orbit coupling: Cobaltates

It is well known^{68), 4), 6)} that in t_{2g} orbital systems a conventional spin-orbit coupling $\lambda(\vec{S} \cdot \vec{l})$ may sometimes play a crucial role in lifting the orbital degeneracy, particularly in case of late-transition metal ions with large λ . When it dominates over the superexchange and weak orbital-lattice interactions, the spin and orbital degrees of freedom are no longer separated, and it is more convenient to formulate the problem in terms of the total angular momentum. Quite often, the spin-orbit ground state has just the twofold Kramers degeneracy, and low-energy magnetic interactions can be mapped on the pseudospin one-half Hamiltonian. This greatly reduces the (initially) large spin-orbital Hilbert space. But, as there is “no free lunch”, the pseudospin Hamiltonians obtain a nontrivial structure, because the bond directionality and frustrations of the orbital interactions are transferred to the pseudospin

sector via the spin-orbital unification. Because of its composite nature, ordering of pseudospin necessarily implies both \vec{S} - and \vec{l} -orderings, and the “ordered” orbital in this case is a complex function. Via its orbital component, the pseudospin order pattern is rather sensitive to the lattice geometry.

Experimental indications for such physics are as follows: (i) a separate JT-structural transition is suppressed but a large magnetostriction effects occur upon magnetic ordering; (ii) effective g -values in the ground state may deviate from the spin-only value and are anisotropic in general; (iii) magnetic order may have a complicated nontrivial structure because of the non-Heisenberg symmetry of pseudospin interactions. As an example, the lowest level of Co^{2+} ions ($t_{2g}^5 e_g^2$, $S = 3/2$, $l = 1$) in a canonical Mott insulators CoO and KCoF_3 is well described by a pseudospin one-half.⁶⁸⁾ Low-energy spin waves in this pseudospin sector, which are separated from less dispersive local transitions to the higher levels with different total momentum, have been observed in neutron scattering experiments in KCoF_3 .⁶⁹⁾

In this section, we apply the pseudospin approach to study the magnetic correlations for the triangular lattice of CoO_2 planes, in which the $\text{Co}^{4+}(t_{2g}^5)$ ions interact via the $\sim 90^\circ$ Co-O-Co bonds. We derive and analyze the exchange interactions in this system, and illustrate how a spin-orbit coupling leads to unusual magnetic correlations. This study is motivated by recent interest in layered cobalt oxides Na_xCoO_2 which have a complex phase diagram including superconductivity, charge and magnetic orderings.⁷⁰⁾

The CoO_2 layer consists of edge sharing CoO_6 octahedra slightly compressed along the trigonal ($c \parallel [111]$) axis. Co ions form a 2D triangular lattice, sandwiched by oxygen layers. It is currently under debate,⁷¹⁾ whether the undoped CoO_2 layer (not yet studied experimentally) could be regarded as Mott insulator or not. Considering the strongly correlated nature of the electronic states in doped cobaltates as is supported by numerous magnetic, transport and photoemission measurements, we assume that the undoped CoO_2 plane is on the insulating side or near the borderline. Thus the notion of spin-charge energy scale separation and hence the superexchange picture is valid at least locally.

5.1. Superexchange interaction for pseudospins

A minimal model for cobaltates should include the orbital degeneracy of the Co^{4+} -ion,⁷²⁾ where a hole in the $d^5(t_{2g})$ shell has the freedom to occupy one out of three orbitals $a = d_{yz}$, $b = d_{xz}$, $c = d_{xy}$. The degeneracy is partially lifted by trigonal distortion, which stabilizes A_{1g} electronic state $(a+b+c)/\sqrt{3}$ over E'_g -doublet $(e^{\pm i\phi}a + e^{\mp i\phi}b + c)/\sqrt{3}$ (hereafter $\phi = 2\pi/3$):

$$H_\Delta = \Delta[n(E'_g) - 2n(A_{1g})]/3. \quad (5.1)$$

The value of Δ is not known; Ref. 72) estimates it $\Delta \sim 25$ meV. Physically, Δ should be sample dependent thus being one of the control parameters. We will later see that magnetic correlations are indeed very sensitive to Δ .

In terms of the effective angular momentum $l = 1$ of the t_{2g} -shell, the functions A_{1g} and E'_g correspond to the $|l_z = 0\rangle$ and $|l_z = \pm 1\rangle$ states, respectively. Therefore, a hole residing on the E'_g orbital doublet will experience an unquenched spin-orbit

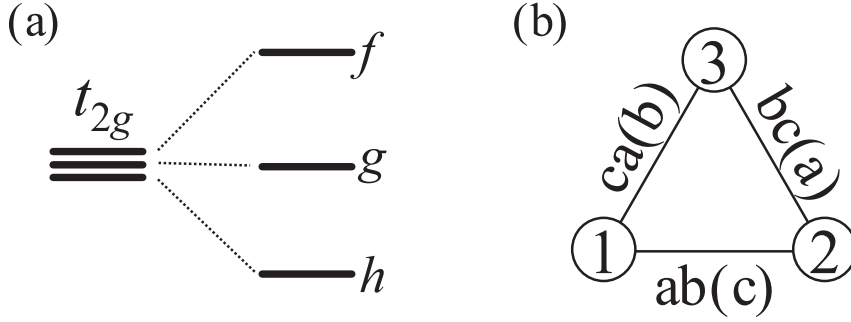


Fig. 4. (a) The t_{2g} -orbital degeneracy of $\text{Co}^{4+}(d^5)$ -ion is lifted by trigonal distortion and spin-orbit interaction. A hole with pseudospin one-half resides on the Kramers f -doublet. Its wavefunction contains both E'_g and A_{1g} states mixed up by spin-orbit coupling. (b) Hopping geometry on the triangular lattice of Co-ions. $\alpha\beta(\gamma)$ on bonds should be read as $t_{\alpha\beta} = t$, $t_{\gamma\gamma} = -t'$, and $\alpha, \beta, \gamma \in \{a, b, c\}$ with $a = d_{yz}$, $b = d_{xz}$, $c = d_{xy}$. The orbital nondiagonal t -hopping stems from the charge-transfer process via oxygen ions, while t' stands for the hopping between the same orbitals due to either their direct overlap or via two intermediate oxygen ions involving t_{pp} . (After Ref. 74).)

interaction $H_\lambda = -\lambda(\vec{S} \cdot \vec{l})$. The coupling constant λ for a free Co^{4+} ion is $650 \text{ cm}^{-1} \approx 80 \text{ meV}$ ⁷³⁾ (this may change in a solid due to the covalency effects).

The Hamiltonian $H = H_\Delta + H_\lambda$ is diagonalized by the following transformation:⁷⁴⁾

$$\alpha_\sigma = i[c_\theta e^{-i\sigma\psi_\alpha} f_{-\bar{\sigma}} + i s_\theta f_{\bar{\sigma}} + e^{i\sigma\psi_\alpha} g_{\bar{\sigma}} + s_\theta e^{-i\sigma\psi_\alpha} h_{-\bar{\sigma}} - i c_\theta h_{\bar{\sigma}}] / \sqrt{3}, \quad (5.2)$$

where $c_\theta = \cos \theta$, $s_\theta = \sin \theta$, $\alpha = (a, b, c)$ and $\psi_\alpha = (\phi, -\phi, 0)$, correspondingly. The angle θ is determined from $\tan 2\theta = 2\sqrt{2}\lambda/(\lambda + 2\Delta)$. As a result, one obtains three levels, $f_{\bar{\sigma}}, g_{\bar{\sigma}}, h_{\bar{\sigma}}$ [see Fig. 4(a)], each of them are Kramers doublets with pseudospin one-half $\bar{\sigma}$. The highest, f -level, which accommodates a hole in d^5 configuration, is separated from the g -level by $\varepsilon_f - \varepsilon_g = \lambda + \frac{1}{2}(\lambda/2 + \Delta)(1/\cos 2\theta - 1)$. This splitting is $\sim 3\lambda/2$ at $\lambda \gg \Delta$, and $\sim \lambda$ in the opposite limit. It is more convenient to use a hole representation, in which the level structure is reversed such that f -level is the lowest one. It is important to observe that the pseudospin $f_{\bar{\sigma}}$ states

$$\begin{aligned} |\bar{\uparrow}\rangle_f &= i c_\theta | +1, \downarrow \rangle - s_\theta | 0, \uparrow \rangle, \\ |\bar{\downarrow}\rangle_f &= i c_\theta | -1, \uparrow \rangle - s_\theta | 0, \downarrow \rangle \end{aligned} \quad (5.3)$$

are coherent mixture of different orbital and spin states. This will have important consequences for the symmetry of intersite interactions.

We assume the hopping Hamiltonian suggested by the edge-shared structure:

$$H_t^{ij} = t(\alpha_{i\sigma}^\dagger \beta_{j\sigma} + \beta_{i\sigma}^\dagger \alpha_{j\sigma}) - t' \gamma_{i\sigma}^\dagger \gamma_{j\sigma} + \text{h.c.}, \quad (5.4)$$

where $t = t_\pi^2/\Delta_{pd}$ originates from d - p - d process via the charge-transfer gap Δ_{pd} , and $t' > 0$ is given either by direct d - d overlap or generated by indirect processes like d - p - d . On each bond, there are two orbitals active in the d - p - d process, while the

third one is transferred via the t' -channel [Fig. 4(b)]. For simplicity, we assume $t' < t$ and neglect t' for a while.

There are three important superexchange processes: **(a)** Two holes meet each other at the Co-site; the excitation energy is U_d . **(b)** Two holes meet each other at an intermediate oxygen-site; the excitation energy $2\Delta_{pd} + U_p$. **(c)** The oxygen electron is transferred to an unoccupied e_g shell and polarizes the spin of the t_{2g} level via the Hund's interaction, $-2J_H(\vec{s}_e \cdot \vec{s}_t)$. This process is important because the $e_g - p$ hopping integral t_σ is larger than t_π . The process (b), termed "a correlation effect" by Goodenough,⁴⁾ is expected to be stronger than contribution (a), as cobaltates belong to the charge-transfer insulators.⁷⁵⁾

These three virtual charge fluctuations give the following contributions:

$$\text{(a)} : \quad A(\vec{S}_i \cdot \vec{S}_j + 1/4)(n_{ia}n_{jb} + n_{ib}n_{ja} + a_i^\dagger b_i a_j^\dagger b_j + b_i^\dagger a_i b_j^\dagger a_j), \quad (5.5)$$

$$\text{(b)} : \quad B(\vec{S}_i \cdot \vec{S}_j - 1/4)(n_{ia}n_{jb} + n_{ib}n_{ja}), \quad (5.6)$$

$$\text{(c)} : \quad -C(\vec{S}_i \cdot \vec{S}_j)(n_{ic} + n_{jc}), \quad (5.7)$$

where $A = 4t^2/U_d$, $B = 4t^2/(\Delta_{pd} + U_p/2)$ and $C = BR$, with $R \simeq (2J_H/\Delta_{pd})(t_\sigma/t_\pi)^2$; $R \sim 1.5\text{--}2$ might be a realistic estimation. [As usual, the orbitals involved depend on the bond direction, and the above equations refer to the 1-2 bond in Fig. 4(b)]. The first, A -contribution can be presented in a $SU(4)$ form (3.15) like in titanites and may have ferromagnetic as well as antiferromagnetic character in spin sector depending on actual orbital correlations. While the second (third) contribution is definitely antiferromagnetic (ferromagnetic). As the constants $A \sim B \sim C \sim 20\text{--}30$ meV are smaller than spin-orbit splitting, we may now *project* the above superexchange Hamiltonian *onto the lowest Kramers level f* , obtaining the effective low-energy interactions between the pseudospins one-half \vec{S}_f . Two limiting cases are presented and discussed below.

Small trigonal field, $\Delta \ll \lambda$. — The pseudospin Hamiltonian has the most symmetric form when the quantization axes are along the Co-O bonds. For the Co-Co pairs 1-2, 2-3 and 3-1 [Fig. 4(b)], respectively, the interactions read as follows:

$$\begin{aligned} H(1-2) &= J_{eff}(-S_i^x S_j^x - S_i^y S_j^y + S_i^z S_j^z), \\ H(2-3) &= J_{eff}(-S_i^y S_j^y - S_i^z S_j^z + S_i^x S_j^x), \\ H(3-1) &= J_{eff}(-S_i^z S_j^z - S_i^x S_j^x + S_i^y S_j^y), \end{aligned} \quad (5.8)$$

where $J_{eff} = 2(B + C)/9 \sim 10\text{--}15$ meV. Here, we denoted the f -pseudospin simply by \vec{S} . Interestingly, the A -term (5.5) does not contribute to the f -level interactions in this limit. The projected exchange interaction is anisotropic and also strongly depends on the bond direction, reflecting the spin-orbital mixed character of the ground state wave function, see Eq. (5.3). Alternation of the antiferromagnetic component from the bond to bond, superimposed on the frustrated nature of a triangular lattice, makes the Hamiltonian (5.8) rather nontrivial and interesting. Surprisingly, one can gauge away the minus signs in Eqs. (5.8) in all the bonds *simultaneously*. To this end, we introduce *four* triangular sublattices, each having a doubled lattice parameter $2a$. The first sublattice includes the origin, while the others are shifted

by vectors $\vec{\delta}_{12}$, $\vec{\delta}_{23}$ and $\vec{\delta}_{31}$ [1,2,3 refer to the sites shown in Fig. 4(b)]. Next, we introduce a fictitious spin on each sublattice (except for the first one), \vec{S}' , which are obtained from the original f -pseudospins \vec{S} by changing the sign of two appropriate components, depending on sublattice index [this is a similar trick, used in the context of the orbital Hamiltonian (3.5) for ferromagnetic YTiO₃; see for details Refs. 21) and 22)]. After these transformations, we arrive at very simple result for the fictitious spins: $H = J_{eff}(\vec{S}'_i \cdot \vec{S}'_j)$ in *all the bonds*. Thus, the known results^{76), 77)} for the AF-Heisenberg model on triangular lattice can be used. Therefore, we take 120°-ordering pattern for the fictitious spins and map it back to the original spin space. The resulting magnetic order has a large unit cell shown in Fig. 5. [Four sublattices have been introduced to map the model on a fictitious spin space; yet each sublattice contains three different orientations of \vec{S}']. Ferro- and antiferromagnetic correlations are mixed up in this structure, and the first ones are more pronounced as expected from Eq. (5.8). Magnetic order is highly noncollinear and also noncoplanar, and a condensation of the spin vorticity in the ground state is apparent. The corresponding Bragg peaks are obtained at positions $K/2 = (2\pi/3, 0)$, that is, half-way from the ferromagnetic Γ -point to the AF-Heisenberg K -point. Because of the “hidden” symmetry (which becomes explicit and takes the form of a global $SU(2)$ for the fictitious spins \vec{S}'), the moments can be rotated at no energy cost. [Note that the “rotation rules” for the real moments are not that simple as for \vec{S}' : they are obtained from a global $SU(2)$ rotation of \vec{S}' via the mapping $\vec{S} \iff \vec{S}'$]. Thus, the excitation spectrum is gapless (at $\Delta = 0$), and can in fact be obtained by folding of the spinwave dispersions of the AF-Heisenberg model. We find nodes at

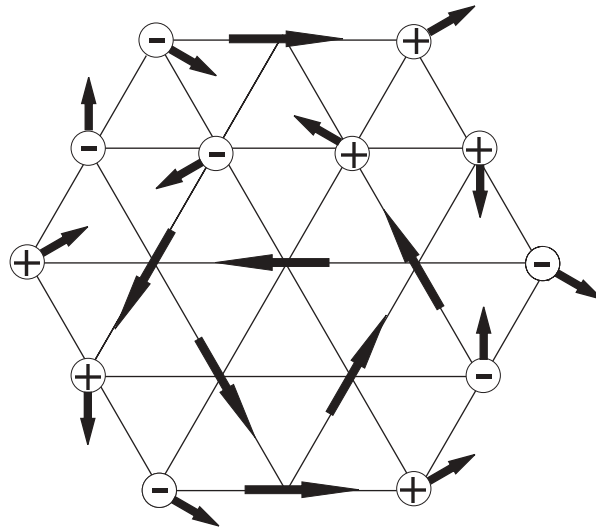


Fig. 5. Expected magnetic ordering in undoped CoO₂ plane in the limit of a small trigonal field. Shown is the magnetic unit cell which contains twelve different lattice sites. Circles with \pm sign indicate the out-of-plane component of the magnetic moment canted away from the plane by an angle θ (with $\tan \theta = \pm\sqrt{2}$). Associated Bragg spots in a momentum space are located at $K/2 = (2\pi/3, 0)$ and equivalent points. (No Bragg intensity at K points.) Note that correlations in a majority of the bonds are more “ferromagnetic” rather than “antiferromagnetic”.

the Bragg points $K/2$ (and also at Γ , K , M points, but magnetic excitations have a vanishing intensity at this points). Spin-wave velocity is $v = (3\sqrt{3}/2)J_{eff}$. A doped-hole motion in such spin background should be highly nontrivial — an interesting problem for a future study.

Large trigonal field, $\Delta \gg \lambda$. — In this case, a natural quantization axes are the in-plane (ab) and out-of-plane (c) directions. The low energy magnetic Hamiltonian obtained reads as follows:

$$H(\Delta \gg \lambda) = J_c S_i^z S_j^z + J_{ab}(S_i^x S_j^x + S_i^y S_j^y), \quad (5.9)$$

with $J_c = [A - 2(3R - 1)B]/9$ and $J_{ab} = (A - B)/9$. As $A \sim B$ and $R > 1$, we have a large negative J_c and small J_{ab} (ferromagnetic Ising-like case). Thus, the *large compression* of CoO_2 plane stabilizes a uniaxial *ferromagnetic state* with moments aligned along the c direction, and the excitations have a gap. When the AF coupling between the different planes is included, expected magnetic structure is then of A -type (ferro- CoO_2 planes coupled antiferromagnetically).

The above results show that the nature of magnetic correlations is highly sensitive to the trigonal distortion. This is because the variation of the ratio λ/Δ strongly modifies the wave-function of the lowest Kramers doublet, which determines the anisotropy of intersite exchange interactions. In this context, it is tempting to mention recent NMR-reports on the observation of magnetic correlations in superconducting cobaltates at wave vectors “in between” the ferromagnetic and AF 120-degree modes,⁷⁸⁾ while correlations change towards the ferromagnetic point in samples with a larger trigonal splitting.⁷⁹⁾ These observations can naturally be understood within the theory presented here, assuming that the Na-doped compounds still “remember” a local magnetic interactions that we obtained here for the insulating limit.

Pseudofermion pairing. — Another interesting point is that unusual superexchange interactions in CoO_2 layer may have important consequences for the pairing symmetry in doped compounds, as argued recently in Ref. 74). Because of the non-Heisenberg form of the effective J -Hamiltonian, usual singlet/triplet classification is not very appropriate. To visualize a symmetry of two paired spins — in the spirit of the RVB picture — we represent the exchange Hamiltonian (5.8) in terms of f -fermionic spinons corresponding to the lowest Kramers doublet. Choosing now quantization along $z \parallel c$, we find

$$H_{ij} = -J_{eff} \Delta_{ij}^{(\gamma)\dagger} \Delta_{ij}^{(\gamma)}, \quad \Delta_{ij}^{(\gamma)} = (t_{ij,0} + e^{i\phi^{(\gamma)}} t_{ij,1} + e^{-i\phi^{(\gamma)}} t_{ij,-1})/\sqrt{3}. \quad (5.10)$$

Here, $t_{ij,0} = i(f_{i\uparrow} f_{j\downarrow} + f_{i\downarrow} f_{j\uparrow})/\sqrt{2}$, $t_{ij,1} = f_{i\uparrow} f_{j\uparrow}$ and $t_{ij,-1} = f_{i\downarrow} f_{j\downarrow}$ correspond to different projections $M = 0, \pm 1$ of the total pseudospin $S_{tot} = 1$ of the pair. The phase $\phi^{(\gamma)}$ in Eq. (5.10) depends on the $\langle ij \rangle$ -bond direction: $\phi^{(\gamma)} = (0, \phi, -\phi)$ for (12, 23, 13)-bonds [see Fig. 4(b)], respectively. As is evident from Eq. (5.10), the pairing field $\Delta_{ij}^{(\gamma)}$ is *spin symmetric but nondegenerate*, because it is made of a particular linear combination of $M = 0, \pm 1$ components, and the total spin of the pair is in fact quenched in the ground state. The absence of degeneracy is due to the fact that the pairing J -interaction has no rotational $SU(2)$ symmetry. In a sense

of spin non-degeneracy, the pair is in a singlet state, although its wavefunction is composed of $M = 0, \pm 1$ states and thus *spin symmetric*. [For the *fictitious* spins introduced above, this would however read antisymmetric.] When such unusual pairs do condense, a momentum space wave-function must be of *odd symmetry* (of p, f, \dots -wave character; a precise form of the gap functions is given in Ref. 74)). It is interesting to note, that the magnetic susceptibility (and hence the NMR Knight shift) is *partially* suppressed in *all three directions* in this paired state. [We recall that \vec{S} represents a total moment of the lowest Kramers level; but no Van Vleck contribution is considered here.] The relative weights of different M -components, which control the Knight-shift anisotropy, depend on trigonal distortion via the ratio Δ/λ , see for details Ref. 74).

5.2. Spin/orbital polarons in a doped NaCoO₂

Finally, we discuss an interesting consequence of the orbital degeneracy in sodium-rich compounds Na_{1-x}CoO₂ at small x . They are strongly correlated metals and also show magnetic order of A -type, which seems surprising in view of the fact that only a small number x of magnetic Co⁴⁺ ions are present (in fact, magnetism disappears for large x). The parent compound NaCoO₂ is usually regarded as a band insulator, as Co³⁺ ions have a spinless configuration t_{2g}^6 . However, one should note that this state results from a delicate balance between the e_g - t_{2g} crystal field splitting and a strong intraatomic Hund's interaction, and a control parameter $10Dq - 2J_H$ may change sign even under relatively weak perturbations. This would stabilize either $t_{2g}^5 e_g$ or $t_{2g}^4 e_g^2$ magnetic configurations, bringing thereby Mott physics "hidden" in the ground state configuration. Doping of NaCoO₂ (by removing Na) is a very efficient way of doing it: a doped charge on Co⁴⁺ sites breaks locally the cubic symmetry and hence splits the e_g and t_{2g} levels on neighboring Co³⁺ sites. This reduces the gap between the lowest level of the split e_g doublet and the upper level of the t_{2g} triplet, favoring a $t_{2g}^5 e_g$ ($S = 1$) configuration.⁸⁰⁾ As a result, a doped charge Co⁴⁺ is dressed by a hexagon of spin-and-orbitally polarized Co³⁺ ions, forming a local object which can be termed as a spin/orbital polaron. The idea of orbital polarons has been proposed and considered in detail in Ref. 81) in the context of weakly doped LaMnO₃. The e_g level splitting on sites next to a doped hole has been estimated to be as large as ~ 0.6 eV (in a perovskite structure with 180°-bonds), leading to a large binding energies and explaining the insulating nature of weakly doped ferromagnetic manganites.

In fact, doping induced spin-state transmutations have been observed in perovskite LaCoO₃,⁸²⁾ in which a small amount of Sr impurities triggers magnetism. Because of their nontrivial magnetic response to the doping, we may classify NaCoO₂ and LaCoO₃ as Mott insulators with *incipient* magnetism. Indeed, a ground state with a filled t_{2g} shell looks formally similar to that of band insulator but is qualitatively different from the latter: NaCoO₂ and LaCoO₃ have low-lying magnetic states. In LaCoO₃, they are just ~ 10 meV above the ground state. Thus, the spin and charge energy scales are completely different. In fact, Co³⁺ ions in LaCoO₃ fully retain their atomic-like multiplet structure, as it is well documented by ESR⁸³⁾ and inelastic neutron scattering⁸⁴⁾ measurements. Spin states of such a Mott insulator

can easily be activated by doping, temperature, etc.

The next important point is that the internal spin structure of the spin/orbital polarons in NaCoO₂ is very different from that in perovskites LaCoO₃ and LaMnO₃. In the latter cases, polarons have a large spin due to internal motion of the bare hole within the polaron (*local* double-exchange process).⁸¹⁾ We argue now that *due to 90°-geometry* of Co-O-Co bonds in NaCoO₂, the exchange interactions within a polaron are strongly antiferromagnetic, and thus a *polaron has a total spin one-half* only. (i) Consider first a superexchange between Co³⁺ ions that surround a central Co⁴⁺ and form a hexagon. They are coupled to each other via the 90°-superexchange. An antiferromagnetic interaction $\tilde{J}(\vec{S}_i \cdot \vec{S}_j)$ between two neighboring Co³⁺ spins ($S = 1$) is mediated by virtual hoppings of electron between t_{2g} and e_g orbitals, $\tilde{t} = t_\sigma t_\pi / \Delta_{pd}$, and we find $\tilde{J} \sim \tilde{t}^2 / E$, where E is a relevant charge excitation energy (order of U_d or $\Delta_{pd} + U_p/2$). Note that there will be also a weaker contribution from t_{2g} - t_{2g} hoppings (antiferromagnetic again) and some ferromagnetic corrections from the Hund's interaction ($\propto J_H/U$), which are neglected. Considering $\tilde{t} \sim 0.2$ eV and $E \sim 3$ eV, we estimate \tilde{J} could be as large as 10–15 meV. Below this energy scale, spins $S = 1$ of Co³⁺-hexagon form a singlet and are thus “hidden”, but they do contribute to the high-temperature magnetic susceptibility in a form $C/(T-\theta)$ with a negative $\theta \sim -\tilde{J}$. (ii) Next, one may think that the double exchange process between the t_{2g} $S = 1/2$ of the central Co⁴⁺ and $S = 1$ of the Co³⁺ would stabilize a large-spin polaron, but this is not the case. Surprisingly, this interaction is also of antiferromagnetic character, because there is no direct e_g - e_g transfer (which gives strong ferromagnetic polarons in perovskites with 180°-bonds like LaCoO₃ and LaMnO₃). Instead, there are two nearly equal double-exchange contributions which favor different spin alignment: (A) an e_g electron of Co³⁺ goes to (a singly occupied) t_{2g} level of Co⁴⁺. This process is possible when the Co³⁺-Co⁴⁺ pair is antiferromagnetic. Another process is that (B) a t_{2g} electron of Co³⁺ goes to an empty e_g level of Co⁴⁺, which favors ferromagnetic bond via the Hund's coupling as for the usual double exchange. The hopping amplitude in both cases is just the same, \tilde{t} , but the kinetic energy gain is slightly larger for the antiferromagnetic configuration, because an extra energy $\sim 10Dq$ (somewhat blocking a charge transfer) is involved in the second process. Therefore, the total double exchange within the pair Co³⁺-Co⁴⁺ is *weakly antiferromagnetic* (a small fraction of \tilde{t}). We thus expect that each polaron brings about a free spin one-half in total, which contributes to the low-energy spin ordering. However, a polaron has an *internal* excitations to a multitude of its larger-spin states which, in principle, could be observed by neutron scattering as a nondispersive and broad magnetic modes (in addition to a propagating excitations in a spin one-half polaron sector).

Our overall picture for Na_{1-x}CoO₂ at small x is that of a heavy spin/orbital polaron liquid. When two polarons overlap, their spins one-half are coupled *ferromagnetically* via the mutual polarization of their spin clouds (Co³⁺-hexagons). Therefore, the polaron liquid may develop (itinerant) ferromagnetism within the CoO₂ planes at low temperatures. The polarons may form clusters or charge-ordered patterns (near commensurate fillings) as discussed in Ref. 80). However, the polaron picture breaks down at large doping x , and no magnetism is expected therefore in

sodium-poor compounds. In other words, a heavy-fermion behavior and magnetism of weakly doped NaCoO_2 originate from the spin-state transmutation of Co^{3+} ions near doped holes, resulting in a narrow polaron bands. An apparent paradox of a *large negative* θ seen in susceptibility, and a *small positive* one inferred from spinwave dispersions⁸⁵⁾ is a natural consequence of our picture: The former one reflects strong AF-couplings (active at large T) within the polaron, while the latter stems from a relatively weak ferromagnetic couplings between the spin-one-half polarons at low energy limit, contributing to magnons. The in-plane coupling subtracted from magnons is found to be small (only of the order of the coupling between the planes).^{85),86)} This is because it stems from a residual effective interactions between a *dilute* system of spin-one-half polarons. Our explanation implies that a quasi two-dimensional layered structure of cobaltates should show up in magnetic excitations of the *magnetically dense* compounds close to the undoped parent system CoO_2 . In that limit, we believe that $|J_{ab}/J_c| \gg 1$, just like in a closely related, but *regular* magnet NaNiO_2 with the same crystal and (*A*-type) magnetic structure, where $|J_{ab}/J_c| \sim 15$.⁸⁷⁾ An important remark concerning the magnon gaps: since all the orbital levels are well split within the polaron (lifting the degeneracy by orbital-charge coupling⁸¹⁾), the magnetic moment of the polaron is mostly of the spin origin. Thus, a low-energy magnetic excitations of a polaron liquid should be of the Heisenberg-type, as in fact observed in sodium-rich samples.^{85),86)}

In our view, marked changes in the properties of cobaltates around $\text{Na}_{0.7}\text{CoO}_2$ are associated with a collapse of the polaron picture. In the magnetic sector, this implies a breakdown of dynamical separation on the strong-AF (weak-F) magnetic bonds within (in-between) the polarons, and a uniform distribution of the exchange interactions sets in.

Summarizing results for the magnetic interactions in the two limiting cases considered in this section: — a “pure” CoO_2 and weakly doped NaCoO_2 — we conclude, that the nature of magnetic correlations in cobaltates is very rich and strongly sensitive to the composition. Description in terms of a simple AF-Heisenberg models with a uniform interactions in all the bonds is not sufficient. Depending on the strength of the trigonal distortion and doping level, we find the spin structures ranging from a highly nontrivial one as shown in Fig. 5, to a conventional *A*-type structures. The *A*-type correlations, which would be favored in a sodium-poor sample by large trigonal field, have an uniaxial anisotropy. On the other hand, the *A*-type state in a sodium-rich compounds is isotropic. Besides a conventional magnons, this state may reveal an interesting high-energy response stemming from its “internal” polaron structure.

§6. Summary

We considered several mechanisms lifting the orbital degeneracy, which are based on: (*i*) electron-lattice coupling, (*ii*) the spin-orbital superexchange, and (*iii*) a relativistic spin-orbit coupling. We discussed mostly limiting cases to understand specific features of each mechanism. Reflecting the different nature of underlying forces, these mechanisms usually compete, and this may lead to nontrivial phase diagrams

as discussed for example for YVO_3 . This underlines the important role of the orbital degrees of freedom as a sensitive control parameter of the electronic phases in transition metal oxides.

We demonstrated the power of the “orbital-angle” ansatz in manganites, where the validity of classical orbital picture is indeed obvious because of large lattice distortions. In titanites and vanadates with much less distorted structures, we find that this simple ansatz is not sufficient and the orbitals have far more freedom in their “angle” dynamics. Here, the lattice distortions serve as an important control parameter and are thus essential, but the quantum exchange process between the orbitals becomes a “center of gravity”.

Comparing the e_g and t_{2g} exchange models, we found that the former case is more classical: the e_g orbitals are less frustrated and the order-from-disorder mechanism is very effective in lifting the frustration by opening the orbital gap. In fact, the low-energy fixed point, formed below the orbital gap in e_g spin-orbital models, can qualitatively be well described in terms of classical “orbital-angle” picture. A strong JT nature of the e_g quadrupole makes in reality this description just an ideal for all the relevant energy/temperature scales.

A classical “orbital-angle” approach to the t_{2g} spin-orbital model fails in a fatal way. Here, the orbital frustration can only be resolved by strong quantum disorder effects, and dynamical coupling between the spins and orbitals is at the heart of the problem. This novel aspect of the “orbital physics”, emerged from recent experimental and theoretical studies of pseudocubic titanites, provide a key in understanding unusual properties of these materials, and make the field as interesting as the physics of quantum spin systems. We believe that the ideas developed in this paper should be relevant also in other t_{2g} orbital systems, where the quantum orbital physics has a chance to survive against orbital-lattice coupling.

Unusual magnetic orderings in layered cobaltates, stabilized by a relativistic spin-orbit coupling are predicted in this paper, illustrating the importance of this coupling in compounds based on late-3d and 4d ions. Finally, we considered how the orbital degeneracy can be lifted locally around doped holes, resulting in a formation of spin/orbital polarons in weakly doped NaCoO_2 . The idea of a dilute polaron liquid provides here a coherent understanding of otherwise puzzling magnetic properties.

In a broader context, a particular behavior of orbitals in the reference insulating compounds should have an important consequences for the orbital-related features of metal-insulator transitions under pressure/temperature/composition, e.g. whether they are “orbital-selective”⁸⁸⁾ or not. In case of LaTiO_3 , where the three-band physics is well present already in the insulating state, it seems natural not to expect the orbital selection. On the other hand, the orbital selection by superexchange and/or lattice interactions is a common case in other insulators (e.g., xy orbital selection in vanadates); here, we believe that the “dimensionality reduction” phenomenon — which is so apparent in the “insulating” models we discussed — should show up already in a metallic side, *partially* lifting the orbital degeneracy and hence supporting the orbital-selective transition picture.

Acknowledgements

I would like to thank B. Keimer and his group members for many stimulating discussions, K. Held and O. K. Andersen for the critical reading of the manuscript and useful comments. This paper benefited a lot from our previous work on orbital physics, and I would like to thank all my collaborators on this topic.

References

- 1) M. Imada, A. Fujimori and Y. Tokura, *Rev. Mod. Phys.* **70** (1998), 1039.
- 2) Y. Tokura and N. Nagaosa, *Science* **288** (2000), 462.
- 3) S. Maekawa, T. Tohyama, S. E. Barnes, S. Ishihara, W. Koshibae and G. Khaliullin, "Physics of Transition Metal Oxides", *Springer Series in Solid State Sciences*, vol. 144 (Springer-Verlag, Berlin, 2004).
- 4) J. B. Goodenough, *Magnetism and Chemical Bond* (Interscience Publ., New York-London, 1963).
- 5) J. Kanamori, *J. Phys. Chem. Solids* **10** (1959), 87; *J. Appl. Phys.* **31** (1960), S14.
- 6) K. I. Kugel and D. I. Khomskii, *Sov. Phys. -Usp.* **25** (1982), 231.
- 7) G. Khaliullin and S. Maekawa, *Phys. Rev. Lett.* **85** (2000), 3950.
- 8) G. Khaliullin, *Phys. Rev. B* **64** (2001), 212405.
- 9) For a recent review of the physical properties of perovskites, see J. B. Goodenough, *Rep. Prog. Phys.* **67** (2004), 1915.
- 10) J. S. Griffith, *The Theory of Transition-Metal Ions* (Cambridge University Press, Cambridge, 1961).
- 11) N. N. Kovaleva, A. V. Boris, C. Bernhard, A. Kulakov, A. Pimenov, A. M. Balbashov, G. Khaliullin and B. Keimer, *Phys. Rev. Lett.* **93** (2004), 147204.
- 12) A. J. Millis, *Phys. Rev. B* **53** (1996), 8434.
- 13) L. F. Feiner and A. M. Oleś, *Phys. Rev. B* **59** (1999), 3295.
- 14) G. Khaliullin, P. Horsch and A. M. Oleś, *Phys. Rev. B* **70** (2004), 195103.
- 15) K. Hirota, N. Kaneko, A. Nishizawa and Y. Endoh, *J. Phys. Soc. Jpn.* **65** (1996), 3736. $J_c = 1.21 \pm 0.05$ meV, $J_{ab} = -1.67 \pm 0.02$ meV.
- 16) I. Loa, P. Adler, A. Grzechnik, K. Syassen, U. Schwarz, M. Hanfland, G. Kh. Rozenberg, P. Gorodetsky and M. P. Pasternak, *Phys. Rev. Lett.* **87** (2001), 125501.
- 17) T. Katsufuji, Y. Taguchi and Y. Tokura, *Phys. Rev. B* **56** (1997), 10145.
- 18) B. Keimer, D. Casa, A. Ivanov, J. W. Lynn, M. v. Zimmermann, J. P. Hill, D. Gibbs, Y. Taguchi and Y. Tokura, *Phys. Rev. Lett.* **85** (2000), 3946.
- 19) C. Ulrich, G. Khaliullin, S. Okamoto, M. Reehuis, A. Ivanov, H. He, Y. Taguchi, Y. Tokura and B. Keimer, *Phys. Rev. Lett.* **89** (2002), 167202.
- 20) M. Cwik, T. Lorenz, J. Baier, R. Müller, G. André, F. Bourée, F. Lichtenberg, A. Freimuth, R. Schmitz, E. Müller-Hartmann and M. Braden, *Phys. Rev. B* **68** (2003), 060401.
- 21) G. Khaliullin and S. Okamoto, *Phys. Rev. Lett.* **89** (2002), 167201.
- 22) G. Khaliullin and S. Okamoto, *Phys. Rev. B* **68** (2003), 205109.
- 23) M. Mochizuki and M. Imada, *Phys. Rev. Lett.* **91** (2003), 167203.
- 24) E. Pavarini, S. Biermann, A. Poteryaev, A. I. Lichtenstein, A. Georges and O. K. Andersen, *Phys. Rev. Lett.* **92** (2004), 176403.
- 25) T. Mizokawa and A. Fujimori, *Phys. Rev. B* **54** (1996), 5368.
- 26) H. Sawada, N. Hamada and K. Terakura, *Physica B* **237-238** (1997), 46.
- 27) J. Akimitsu, H. Ichikawa, N. Eguchi, T. Miyano, M. Nishi and K. Kakurai, *J. Phys. Soc. Jpn.* **70** (2001), 3475.
- 28) T. Kiyama and M. Itoh, *Phys. Rev. Lett.* **91** (2003), 167202.
- 29) T. Kiyama, H. Saitoh, M. Itoh, K. Kodama, H. Ichikawa and J. Akimitsu, *J. Phys. Soc. Jpn.* **74** (2005), 1123.
- 30) In fact, the resonant x-ray scattering data shows that the orbital polarization in LaTiO_3 is much weaker than in YTiO_3 : M. Kubota, H. Nakao, Y. Murakami, Y. Taguchi, M. Iwama and Y. Tokura, *Phys. Rev. B* **70** (2005), 245125.
- 31) E. Pavarini, A. Yamasaki, J. Nuss and O. K. Andersen, *New J. Phys.* **7** (2005), 188.
- 32) I. V. Solovyev, *Phys. Rev. B* **69** (2004), 134403.

- 33) G. Keller, K. Held, V. Eyert, D. Vollhardt and V. I. Anisimov, Phys. Rev. B **70** (2004), 205116.
- 34) E. D. Nelson, J. Y. Wong and A. L. Schawlow, Phys. Rev. **156** (1967), 298.
- 35) C. Ulrich, A. Gössling, M. Grüninger, M. Guennou, H. Roth, M. Cwik, T. Lorenz, G. Khaliullin and B. Keimer, cond-mat/0503106.
- 36) Z.-P. Shi and R. R. P. Singh, Phys. Rev. B **52** (1995), 9620.
- 37) S. Miyasaka, T. Okuda and Y. Tokura, Phys. Rev. Lett. **85** (2000), 5388.
- 38) G. Khaliullin, P. Horsch and A. M. Oleś, Phys. Rev. Lett. **86** (2001), 3879.
- 39) C. Ulrich, G. Khaliullin, J. Sirker, M. Reehuis, M. Ohl, S. Miyasaka, Y. Tokura and B. Keimer, Phys. Rev. Lett. **91** (2003), 257202.
- 40) J. Sirker and G. Khaliullin, Phys. Rev. B **67** (2003), 100408(R).
- 41) J.-Q. Yan, J.-S. Zhou and J. B. Goodenough, Phys. Rev. Lett. **93** (2004), 235901.
- 42) G. Khaliullin, (unpublished). The predicted spin couplings for the ferrates are: NN $J_1 \simeq -2.2$ meV, second NN $J_2 \simeq 0.3$ meV, and fourth NN $J_4 \simeq 0.5$ meV.
- 43) A. Lebon, P. Adler, C. Bernhard, A. Boris, A. Pimenov, A. Maljuk, C. T. Lin, C. Ulrich and B. Keimer, Phys. Rev. Lett. **92** (2004), 037202.
- 44) J. van den Brink, P. Horsch, F. Mack and A. M. Oleś, Phys. Rev. B **59** (1999), 6795.
- 45) For a discussion of the order-from-disorder phenomena in frustrated spin systems, see A. M. Tsvelik, *Quantum Field Theory in Condensed Matter Physics* (Cambridge University Press, Cambridge, 1995), Chap. 17, and references therein.
- 46) K. Kubo, J. Phys. Soc. Jpn. **71** (2002), 1308.
- 47) K. I. Kugel and D. I. Khomskii, Sov. Phys. -Solid State **17** (1975), 285.
- 48) Y. Okimoto, T. Katsufuji, Y. Okada, T. Arima and Y. Tokura, Phys. Rev. B **51** (1995), 9581.
- 49) R. Rückamp, E. Benckiser, M. W. Haverkort, H. Roth, T. Lorenz, A. Freimuth, L. Jongen, A. Möller, G. Meyer, P. Reutler, B. Büchner, A. Revcolevschi, S.-W. Cheong, C. Sekar, G. Krabbes and M. Grüninger, New J. Phys. **7** (2005), 144.
- 50) S. Ishihara, Phys. Rev. B **69** (2004), 075118.
- 51) L. F. Feiner, A. M. Oleś and J. Zaanen, Phys. Rev. Lett. **78** (1997), 2799.
- 52) G. Khaliullin and V. Oudovenko, Phys. Rev. B **56** (1997), R14243.
- 53) H. Tsunetsugu and Y. Motome, Phys. Rev. B **68** (2003), 060405(R).
- 54) A. B. Harris, T. Yildirim, A. Aharony, O. Entin-Wohlman and I. Ya. Korenblit, Phys. Rev. Lett. **91** (2003), 087206.
- 55) Y. Q. Li, M. Ma, D. N. Shi and F. C. Zhang, Phys. Rev. Lett. **81** (1998), 3527.
- 56) B. Frischmuth, F. Mila and M. Troyer, Phys. Rev. Lett. **82** (1999), 835.
- 57) H. J. Schulz, Phys. Rev. Lett. **77** (1996), 2790.
- 58) M. Mochizuki and M. Imada, J. Phys. Soc. Jpn. **70** (2001), 1777.
- 59) S. Miyasaka, Y. Okimoto and Y. Tokura, J. Phys. Soc. Jpn. **71** (2002), 2086.
- 60) Y. Motome, H. Seo, Z. Fang and N. Nagaosa, Phys. Rev. Lett. **90** (2003), 146602.
- 61) T. Mizokawa, D. I. Khomskii and G. A. Sawatzky, Phys. Rev. B **60** (1999), 7309.
- 62) Shun-Qing Shen, X. C. Xie and F. C. Zhang, Phys. Rev. Lett. **88** (2002), 027201.
- 63) P. Horsch, A. M. Oleś and G. Khaliullin, Phys. Rev. Lett. **91** (2003), 257203.
- 64) S. Miyashita, A. Kawaguchi, N. Kawakami and G. Khaliullin, Phys. Rev. B **69** (2004), 104425.
- 65) J. Fujioka, S. Miyasaka and Y. Tokura, Phys. Rev. B **72** (2005), 024460.
- 66) S. Ishihara, Phys. Rev. Lett. **94** (2005), 156408.
- 67) M. Ogata and H. Shiba, Phys. Rev. B **41** (1990), 2326.
- 68) J. Kanamori, Prog. Theor. Phys. **17** (1956), 177; *ibid.* **17** (1956), 197.
- 69) T. M. Holden, W. J. L. Buyers, E. C. Svensson, R. A. Cowley, M. T. Hutchings, D. Hukin and R. W. H. Stevenson, J. of Phys. C **4** (1971), 2127.
- 70) M. L. Foo, Y. Wang, S. Watauchi, H. W. Zandbergen, T. He, R. J. Cava and N. P. Ong, Phys. Rev. Lett. **92** (2004), 247001.
- 71) K.-W. Lee and W. E. Pickett, Phys. Rev. B **72** (2005), 115110.
- 72) W. Koshibae and S. Maekawa, Phys. Rev. Lett. **91** (2003), 257003.
- 73) B. N. Figgis and M. A. Hitchman, *Ligand Field Theory and Its Applications* (New York, Wiley-VCH, 2000).
- 74) G. Khaliullin, W. Koshibae and S. Maekawa, Phys. Rev. Lett. **93** (2004), 176401.
- 75) J. Zaanen, G. A. Sawatzky and J. W. Allen, Phys. Rev. Lett. **55** (1985), 418.

- 76) S. J. Miyake, *J. Phys. Soc. Jpn.* **61** (1992), 983.
- 77) L. Capriotti, A. E. Trumper and S. Sorella, *Phys. Rev. Lett.* **82** (1999), 3899.
- 78) F. L. Ning and T. Imai, *Phys. Rev. Lett.* **94** (2005), 227004.
- 79) Y. Ihara, K. Ishida, C. Michioka, M. Kato, K. Yoshimura, K. Takada, T. Sasaki, H. Sakurai and E. Takayama-Muromachi, *J. Phys. Soc. Jpn.* **74** (2005), 867.
- 80) C. Bernhard, A. V. Boris, N. N. Kovaleva, G. Khaliullin, A. V. Pimenov, L. Yu, D. P. Chen, C. T. Lin and B. Keimer, *Phys. Rev. Lett.* **93** (2004), 167003.
- 81) R. Kilian and G. Khaliullin, *Phys. Rev. B* **60** (1999), 13458.
- 82) S. Yamaguchi, Y. Okimoto, H. Taniguchi and Y. Tokura, *Phys. Rev. B* **53** (1996), R2926.
- 83) S. Noguchi, S. Kawamata, K. Okuda, H. Nojiri and M. Motokawa, *Phys. Rev. B* **66** (2002), 094404.
- 84) A. Podlesnyak, S. Streule, J. Mesot, M. Medarde, E. Pomjakushina, K. Conder, M. W. Haverkort and D. I. Khomskii, *cond-mat/0505344*.
- 85) S. P. Bayrakci, I. Mirebeau, P. Bourges, Y. Sidis, M. Enderle, J. Mesot, D. P. Chen, C. T. Lin and B. Keimer, *Phys. Rev. Lett.* **94** (2005), 157205.
- 86) L. M. Helme, A. T. Boothroyd, R. Coldea, D. Prabhakaran, D. A. Tennant, A. Hiess and J. Kulda, *Phys. Rev. Lett.* **94** (2005), 157206.
- 87) M. J. Lewis, B. D. Gaulin, L. Filion, C. Kallin, A. J. Berlinsky, H. A. Dabkowska, Y. Qiu and J. R. D. Copley, *Phys. Rev. B* **72** (2005), 014408.
- 88) A. Koga, N. Kawakami, T. M. Rice and M. Sgrist, *Phys. Rev. B* **72** (2005), 045128.